Contrasting reproductive biology of two hydrothermal gastropods from the Mid-Atlantic Ridge: implications for resilience of vent communities

Marticorena Julien [1, *], Matabos Marjolaine [1], Sarrazin Jozee [1], Ramirez-Llodra E. [2, 3]

[1] REM/EEP, Ifremer, 29280, Plouzané, France
[2] Norwegian Institute for Water Research, Gaustadalleen 21, 0349, Oslo, Norway
[3] REV Ocean, Oksenøyveien 10, 1366, Lysaker, Norway

* Corresponding author : Julien Marticorena, email address : julienmarticorena@gmail.fr

Abstract :

The recovery of populations and their ability to recolonise a disturbed habitat is mainly dependent on their reproductive biology (e.g., fecundity, frequency of reproduction, and time to maturity) and recruitment success. To assess recolonisation processes and connectivity of vent communities, and infer their resilience to natural and anthropogenic disturbances, we studied the life-history traits of two dominant species of vent gastropods from the northern Mid-Atlantic Ridge: Protolira valvatoides and Pseudorimula midatlantica. Gonad morphology, gametogenesis, and reproductive outputs related to shell length were described using histological analyses, and population structure was assessed from individuals' size–frequency distributions. Samples were collected at different locations of the Montségur and Eiffel Tower edifices (Lucky Strike vent field) in April 2015, July 2017, and August 2018 to inform on spatial and temporal variations of their reproductive outputs and demography. All stages of oocyte development were found in the gonads of both species, suggesting a continuous gametogenesis and asynchronous reproduction. However, the two species showed contrasting reproductive strategies. Indeed, while P. midatlantica is gonochoric with a fecundity of up to 327 mature oocytes, P. valvatoides is hermaphrodite with an extremely low fecundity including a maximum of eight vitellogenic oocytes. Maximum oocyte size was 176 μm for P. midatlantica and 272 μm for P. valvatoides. We infer from previous knowledge and our results that both species exhibit a lecithotrophic development of larvae. There was no evidence of temporal variability of reproductive traits, but environmental conditions seem to affect gametogenetic maturity and oocyte size of P. midatlantica limpets. Variations in population structure at the edifice scale suggest habitat selection of individuals related to biotic and abiotic factors.

Introduction

Current worldwide demand in minerals and metals is rising while land-based resources are severely decreasing (Hein et al. 2013). In this context, the interest of companies and countries in deep-sea mining is escalating, targeting various high metal-based environments such as Seafloor Massive Sulphide (SMS) deposits at hydrothermal vents, polymetallic nodules on abyssal plains and cobalt-rich ferromanganese crusts at seamounts (Gollner et al. 2017). Although commercial exploitation of seabed minerals has not yet begun, expected consequences of deep-sea mining on ecosystems comprise direct and indirect impacts that will vary with mining strategies (Ramirez-Llodra et al. 2011; Clark and Smith, 2013; Van Dover, 2014; Levin 2016) as well as with the biological and environmental characteristics of the targeted ecosystems (Gollner 2017). In this context, it is urgent to evaluate the resilience of deep-sea communities to inform the development of environmental management plans.

Resilience can be defined as the ability of an ecosystem to maintain its structure and function in response to a perturbation (Carpenter et al. 2001; Cumming et al. 2012). This definition involves two distinct processes: (1) resistance, related to the ability of a system to absorb the effects of disturbance without changing (Connell and Ghedini 2015) and (2) recovery, which is the capacity of an ecosystem to return to its undisturbed state (Ingrisch and Bahn 2018). Functional resilience occurs at multiple scales of ecological organisation, ranging from individual to community levels (Oliver et al. 2015). At the population-level, resilience refers to the ability of a species to occupy new space and recolonise a disturbed area. It is partly related to reproductive traits such as reproductive frequency, fecundity, time to maturity and recruitment success (see Gladstone-Gallagher et al. 2019). Thus, the recovery of impacted habitats is highly dependent on the dispersal and recolonisation potential of the different species.

Hydrothermal vents represent extremely fragmented and transient habitats that can be separated by tens to hundreds of kilometres along mid-ocean ridges and back-arc basins. Consequently, the recovery of impacted vent communities will strongly depend on larval

71 supply reaching from preserved areas and on the success of recruitment events. Connectivity

72 patterns are major drivers of the demographic stability of local populations. Two

73 complementary methods can help to assess the connectivity between populations: i)

74 population genetic based models (Tyler and Young 1999; Vrijenhoek 2010; Baco et al. 2016)

75 and ii) coupled biophysical models that include ocean circulation and early life-history traits

76 such as timing of spawning, fecundity, larval mortality and planktonic larval duration (Pradillon

77 et al. 2001; Metaxas and Saunders 2009; Hilario et al. 2015; Suzuki et al. 2018; Vic et al. 2018).

78 However, despite their relevance, discrepancies in the results of these modelling approaches

79 highlight a lack of knowledge of both physical and biological variables in deep-sea ecosystems

80 (Breusing et al. 2016). Indeed, for most deep-sea species, empirical data on early life-history

81 traits is, at best, fragmentary but often completely lacking (Tyler and Young 1999). It is

82 therefore urgent to increase our knowledge about the natural processes driving population

83 connectivity, colonisation patterns and ecosystem recovery, to better understand the

84 resilience of vent communities following a disturbance (Mullineaux et al. 2010; Gollner et al.

85 2015; Boschen et al. 2016; Gollner et al. 2017).

86

87 Hydrothermal vent communities in the northern part of the mid-Atlantic ridge and specifically

88 at the Lucky Strike vent field (LS) are characterised by dense assemblages of macrofauna,

89 structured by the engineer species *Bathymodiolus azoricus*. *B. azoricus* mussel beds provide a

90 three-dimensional habitat promoting high-density populations of gastropods (*Protolira*

91 *valvatoides, Pseudorimula midatlantica, Lepetodrilus atlanticus*) and polychaetes

92 (*Branchipolynoe seepensis, Amphisamytha lutzi* (Cuvelier et al. 2014; Sarrazin et al. 2015).

93 While basic reproductive traits are known for most species in the area, only the reproductive

94 biology of *B. azoricus*, *L. atlanticus*, *B. seepensis* and *A. lutzi* has been described in details (Van

95 Dover et al. 1999; Jollivet et al. 2000; Blake and Van Dover 2005; Colaco et al. 2006; Dixon et

96 al. 2006; Tyler et al. 2008), and our knowledge of gastropods remains limited. Gathering this

97 information is key in understanding the establishment of vent faunal communities and

98 ecosystem functioning.

99

100 Gametogenesis, and especially vitellogenetic mechanisms, defined as the synthesis and

4

storage of energetic reserves in the growing oocytes, appears to be phylogenetically constrained (Eckelbarger 1995; Tyler and Young 1999). In contrast, the number and quality of the eggs, and also the time of spawning, can be affected by environmental conditions (Ramirez-Llodra 2002; Kelly and Metaxas 2007; Matabos and Thiebaut 2010). The continuous supply of energy introduced in the food web by chemoautotrophic bacteria at hydrothermal vents can support an asynchronous and quasi-continuous production of eggs by benthic species, but seasonal reproduction has also been observed in bathymodiolin mussels (reviewed by Laming et al. 2018). Energy availability can also shape the trade-off between egg size and fecundity (Ramirez-Llodra 2002), and the size of mature oocytes can provide information about larval development mode and help determining the type of larvae. Planktotrophic larvae are those feeding in the water-column, while lecithotrophic larvae feed on the egg's yolk until settlement. As a general pattern, species producing a large number of small eggs (< 200 μm) have planktotrophic larval feeding modes, while lecithotrophic species produce a small number of larger eggs (> 200 μm) (Jaekle 1995; Levin and Bridges 1995). For molluscs, larval shell morphology has also been used to infer larval development and dispersal, based on observations of shallow-water species (Gustafson and Lutz 1994). *Protolira* species are hermaphroditic and have a spirally coiled propodial appendage interpreted as a penis and thus with assumed pseudo-internal fertilization occurring in the pallial cavity (Warén and Bouchet 1993. *P. midatlantica* (Mclean 1992) is described as gonochoristic and characterized by a hypertrophied gonad that displaces the foot on the left side of the animal, probably in response to the need of a greater reproductive output (Mclean 1992).

In this study, we describe for the first time the gametogenesis, population structure and infer the reproductive output at the time of sampling of two abundant MAR gastropods (*Protolira valvatoides* and *Pseudorimula midatlantica*), providing novel data to better assess the recovery potential of vent ecosystems in face of natural and anthropogenic disturbances. This work is part of a larger study that aims at evaluating the rate and success of recovery of active hydrothermal vent communities after an induced disturbance using a 2 year *in situ* experiment. Community recolonisation one year and two years after disturbance (faunal removal) was monitored and the role of biological and chemical factors on recolonisation dynamics evaluated.

Material and Methods

Field sampling

All specimens of *Protolira valvatoides* and *Pseudorimula midatlantica* were sampled using the hydraulic arm and suction sampling device of the Remotely Operated Vehicle *Victor6000*. They were collected in *Bathymodiolus azoricus* assemblages on diffused flow habitats on the Montségur and Eiffel Tower edifices (Lucky Strike vent field, MAR) at 1700 m depth (Fig. 1). To investigate spatial variation of reproductive and population structure features, samples were collected at different sampling locations with varying environmental conditions (Fig. 1, Table 1). Sample names refer to a disturbance experiment that was held on the Montségur edifice from 2017 to 2019. Individuals from three cruises, occurring in May 2015 (MOMARSAT2015), July 2017 (MOMARSAT2017) and August 2018 (MOMARSAT2018), were compared to test for temporal variations across the two species.

To complete the dataset, *in situ* temperature measurements were conducted year-round with autonomous MISO (2015, WHOI-MISO low temp-ONSET®) and iButtons[TM] (2017 and 2018) probes deployed directly on the mussel assemblages.

On board, all faunal samples were washed on a 300 µm sieve and gastropods were identified to species level. Five to twenty individuals of *P. valvatoides* and *P. midatlantica* from each sample were stored in buffered 4% formaldehyde for reproduction studies, whereas all other specimens were preserved in 96% ethanol for population structure analyses.

Population structure

Size-frequency distributions of both species were only analysed for the samples from the Montségur edifice, as most of the Eiffel Tower specimens were used for other analyses and therefore not measured. To characterize demographic population structure, photos of *P. midatlantica* and *P. valvatoides* were captured with a Leica MC 170 HD camera mounted on a Leica M125 dissecting microscope. The curvilinear distance (i.e. longest length from the apex to the anterior edge of the shell along the dorsal side) of *P. midatlantica* and the longest shell dimension of *P. valvatoides* (see Bates et al. 2006 for protocol) were measured to the nearest 0.001 mm using the Leica Application Suite software. Measurement error was calculated as

6

163 the maximum difference among 10 measures of the same individual on 10 specimens

164 comprising a range of all sizes for each species. It was fixed at 0.052 mm for *P. midatlantica*

165 and 0.029 mm for *P. valvatoides*.

166 For each assemblage sampled, length-frequency distribution was plotted for the two species

167 using a size-class interval of 0.3 mm for *P. midatlantica* and 0.2 mm for *P. valvatoides*. The

168 intervals were chosen according to three criteria: i) most size-classes must have at least five

169 individuals; ii) the number of adjacent empty classes must be minimized; and iii) the interval

170 has to be much greater than the measurement error (see Jollivet et al. 2000). Size-frequency

171 distributions were compared to a normal distribution using a one-sample Kolmogorov-

172 Smirnov test and non-parametric Kruskal-Wallis multisample tests were performed to identify

173 differences in size-frequency distribution between samples. To determine which individuals

174 contributed to the observed differences, multiple comparison Nemenyi and Dunn tests were

175 computed (Zar, 2007).

176

177 When distributions differed significantly from a normal distribution, and assuming that

178 gastropod sizes followed a Gaussian distribution within each cohort, a modal decomposition

179 was ran for all sampled assemblages of *P. valvatoides*. Modal decomposition analyses were

180 not performed for *P. midatlantica* because at least 100 to 300 specimens are required to have

181 a fairly good representation of the population, which was not the case in some of our samples

182 for this species. The modal decomposition analyses of *P. valvatoides* was conducted with the

183 Mixdist package (Macdonald and Du, 2018) in R (RStudio Team, 2016), which identifies the

184 total number of cohorts within the natural distribution and calculates the mean size, standard

185 deviation and proportion of the overall population in each cohort. The goodness of fit of

186 identified size cohorts was verified using a chi-squared test. Seven individuals of *P. valvatoides*

187 were removed from the distribution of C1a, C1acg and R1 before the MIX analysis to avoid

188 null classes separating the modes.

189

190

Reproductive biology

The shells of *P. midatlantica* were gently removed using forceps, while *P. valvatoides* individuals were rapidly decalcified using a HCL 10% solution before removing the periostracum under a dissecting microscope. The entire soft body was then processed through graded ethanol and dehydrated in absolute isopropanol before being embedded in paraffin wax. For histological analyses, serial horizontal 7 µm thick sections of gonads were prepared using a microtome. Sections were stained with the routine staining haematoxylin and eosin protocol (Gabe, 1968). Observations were performed using the AxioZoom stereomicroscope (Zeiss, Oberkochen, Germany) equipped with an ApoTome.2 slider module (Zeiss) and a HXP 200C light technology (Zeiss) and using an AxioCam MRm (Zeiss) camera. Micrographs were analyzed using the Zen (Zeiss) software.

For gametogenesis studies, at least 100 oocytes per specimen were measured using the image J © software (Schneider et al. 2012) from 2 to 3 serial sections for *P. midatlantica.* For *P. valvatoides,* the very low number of oocytes was insufficient to reach 100 oocytes even when using serial sections of the entire gonad. Only oocytes that had been sectioned through the nucleus were measured using the feret diameter, which estimates the diameter of a hypothetical disc with the same area as the measured object. Oocyte sizes were grouped into 10 µm classes for frequency diagrams constructed for each sampling location. To assess synchrony of gametogenesis among and between samples, non-parametric Kruskal-Wallis multi-sample and Nemenyi and Dunn tests were performed on oocyte size. Gametogenetic maturity was estimated from the percentage of vitellogenic oocytes on the total of oocytes measured for each animal and comparisons among samples were made using the same methods as previously described.

Instantaneous fecundity was quantified as the number of vitellogenic oocytes in the entire ovary of an individual at the time of sampling (Tyler and Billett 1988; Ramirez-Llodra 2002). Fecundity was quantified in 10 individuals for *P. midatlantica* and 9 individuals for *P. valvatoides*. To ensure that a vitellogenic oocyte was not counted more than once, the overlying sections were compared.

8

Results

The mean temperatures measured over the year within the different quadrats varied between 5.1 and 8.3°C and were typical of a diffuse flow venting area (Table 1). Significant spatial variations of mean temperature have been identified with the presence of warmer habitats in R1, C2a and C1a quadrats (ANOVA, F = 6591, p-value < 0.001).

Gonad morphology and gametogenesis

In total, 58 individuals of *Protolira valvatoides* and 34 females of *Pseudorimula midatlantica*, collected at different sampling locations, over three years, were analyzed (Table 1).

The hermaphroditic genital system of *Protolira valvatoides* consists of separate ovary with oviduct and a testis with a *vas deferens* (Fig. 2a and c). The large ovary is situated dorsally and occupies, together with the digestive gland, the uppermost whorl of the shell (Fig. 2a and c). The testis is located anterio-ventrally of the ovary, extending on the right side of the animal. Spermatogenesis begins with the development of germinal spermatogonia with a mean diameter of 4 μm from the wall of testis tubules. Spermatogonia differentiate in spermatocytes and spermatids *via* mitotic divisions, before developing into flagellated spermatozoa in the lumen of the testis (Fig. 2g). During oogenesis, the oogonia proliferate in the germinal epithelium, which extends throughout the entire ovary. Oogonia grow to approximatively 20 μm before developing in previtellogenic oocytes. Oogonia appear in histological sections as small cells with a large and dark stained nucleus occupying the entire cell, while previtellogenic oocytes are larger (20–100 μm) with a basophilic and more voluminous cytoplasm that stain in light purple (Fig. 2e). Previtellogenic oocytes grow until reaching 80–100 μm, when they undergo vitellogenesis. At the beginning of vitellogenesis, yolk granules are visible at the periphery of the oocytes and spread to the entire oocyte. Vitellogenic oocytes show an eccentric germinal vesicle and acidophilic cytoplasm stained in pale pink with eosin (Fig. 2e). For *Protolira valvatoides*, the mean size of vitellogenic oocytes was 185 μm (ferret diameter) and the maximum size measured was 272 μm.

253   *Pseudorimula midatlantica* is a gonochoric species with separated male and female
254   individuals. In females, the ovary occupies a large volume of the animal, extending from the
255   very posterior end to the pallial roof on the right side (Fig. 2b). It is ventrally replaced by the
256   stomach and digestive glands and surrounded on both sides by the shell muscle (Fig. 2d). The
257   development and maturation of oocytes and spermatozoa are similar to *P. valvatoides* (Fig.
258   2H). In the ovary, the previtellogenic oocytes grow to a size of 40–50 µm before starting
259   vitellogenesis (Fig. 2f). The mean size of vitellogenic oocyte for *P. midatlantica* was 81 µm,
260   with a maximum size of 176 µm, and yolk was distributed all over the oocyte (Fig. 2f). All
261   developmental stages of oocytes (i.e. oogonia, previtellogenic oocytes and vitellogenic
262   oocytes) were observed in all individuals analysed for both species.

263

264   *Oocyte size-frequency distribution*
265   For both species, oogonia were much more abundant in ovaries than previtellogenic and
266   vitellogenic oocytes. Hence, oogonia were not considered for oocyte-size distribution
267   analyses. For both species, the Kruskal-Wallis multisample test showed intra-sample
268   differences in mean oocytes size and the post-hoc Dunn's multi-sample test indicated that
269   only one to three individuals of each sample contributed to these differences (Table S1). To
270   ensure that there was no individual size effect among samples in testing the spatial and
271   temporal variation of oocyte distribution, we compared shell length of the examined
272   individuals. No significant differences were identified (Test Kruskal-Wallis, $H = 0.44$, df = 7, p-
273   value > 0.05 for *P. valvatoides* and $H = 11.07$, df = 7, p-value > 0.05 for *P. midatlantica*). Oocyte
274   size-frequency distributions were highly variable between individuals and there was no
275   evidence of synchronous oogenesis. However, the two species displayed the same polymodal
276   pattern in oocyte-frequency distribution skewed towards smaller oocytes with a tail in larger
277   sizes that may contain several modes (Figs. 3 and 4).

278

279   For *P. valvatoides*, oocyte size ranged from 9 to 272 µm (Fig. 3) and the size-frequency
280   distribution showed a first peak containing between 91 and 96 % of the total number of
281   oocytes, corresponding to previtellogenic oocytes (< 100 µm). The rest of the distribution
282   contained one or more peaks of larger oocytes (> 100 µm), corresponding to previtellogenic
283   oocytes at the onset of vitellogenesis and truly vitellogenic oocytes. Kruskal-Wallis multi-
284   sample tests showed that oocytes size distributions between locations and sampling period

285 did not differ significantly (Fig. 5a and c, Fig. S1). The percentage of mature oocytes ranged

286 from 3% to 18% of all oocytes and was not correlated with the animal body length (R^2 = -0.014,

287 p-value = 0.91) (Fig. 6a). Finally, no difference was observed regarding the proportion of

288 vitellogenic oocytes among localities (Kruskal-Wallis test, H = 7.23, df = 5, p-value > 0.05; Fig.

289 5c)

290

291 For *P. midatlantica,* oocyte size ranged from 4 to 176 µm (Fig. 4) and size frequency

292 distribution showed a first peak, containing between 31 and 82 % of the total population,

293 which corresponded to previtellogenic oocytes (< 50 µm). A second and minor peak was

294 mostly constituted by larger vitellogenic oocytes (> 50 µm). An intermediate peak including

295 oocytes at the beginning of vitellogenesis (between 40 and 50 µm) was also present for most

296 of the localities (Fig. 4). *P. midatlantica* showed a significant spatial variation in oocyte size

297 distribution among the different sites with smaller oocytes in the C1a sample and larger

298 oocytes in the C2a sample (Fig. 5b and d). Nevertheless, there was no evidence of temporal

299 variation in mean oocyte size of *P. midatlantica* (Fig. S2). For this species, the percentage of

300 mature oocytes was independent of body size and ranged from 6% to 51% of all oocytes (Fig.

301 6B). The percentage of mature oocytes varied significantly among localities, with a larger

302 proportion of vitellogenic oocytes in the C2a and R1 samples (Kruskal-Wallis test, H = 19.43,

303 df = 6, p-value < 0.005).

304

305 *Fecundity*

306 An estimation of instantaneous fecundity was measured from individuals randomly selected

307 among the C1a sample. In total, 9 individuals of *P. valvatoides* with sizes ranging from 2.2 to

308 3.4 mm, and 10 females of *P. midatlantica,* with shell lengths comprised between 4.1 and 8

309 mm, were analysed. In this study, even the smallest individuals examined possessed

310 vitellogenic oocytes, so it was not possible to assess the minimal size at first maturity.

311 Furthermore, for both species, mature individuals with shell length about half of their

312 maximum size have been found. In *P. valvatoides*, the maximum instantaneous fecundity was

313 very low, with only 8 vitellogenic oocytes through the entire ovary. Fecundity appears to be

314 independent of animal size for the 9 individuals analysed (R^2=0.007, p-value = 0.34). Mean

315 instantaneous fecundity of *P. midatlantica* was 187 ± 44 oocytes per female, with a maximum

316 of 327 oocytes found in an individual with a length of 8 mm. Fecundity and shell length showed

317 a positive linear relationship for the 10 examined specimens of *P. midatlantica* (R^2 = 0.84, p-

318 value < 0.001).

319

320 *Population structure*

321 The demographic structures of the two species for each sample collected on Montségur in

322 2017 are presented in Figures 7a and b. All frequency distributions significantly differed from

323 the normal distribution (Kolmogorov-Smirnov test, p-value <0.001) and were thus assumed to

324 be polymodal. For *P. valvatoides*, specimens ranged in shell length from 0.51 to 3.84 mm.

325 Distributions were dominated by large individuals with a major peak between 2 and 2.5 mm

326 (Fig. 7). However, while the chi² tests associated with the MIX modal decomposition

327 highlighted no significant differences between the observed and obtained theoretical

328 distributions, the low level of acceptance did not allow to determine reliable cohorts within

329 the studied population. This might be due to the limited number of individuals analysed, or

330 related to processes other than discontinuous recruitment. The Kruskal-Wallis multi-sample

331 test identified significant differences in size-frequency distribution between the different

332 samples (H = 49.424, df = 3, p-value < 0.001) and the post-hoc Dunn's multi-sample test

333 showed that every sample was different from each other, except for C1acg which is not

334 significantly different from C2a and R1 (Table 2).

335

336 The low abundance of *P. midatlantica* did not allow to perform modal decomposition analysis,

337 but the size distribution is highly variable across the different samples with, for example, a

338 mean size of 2.4 ± 0.7 mm in the C1a sample against 3.7 ± 1.1 mm in C2a. The Kruskal-Wallis

339 multi-sample test confirmed the observed difference among the localities (H = 112.04, df = 6,

340 p-value < 0.001) and the post-hoc multiple Dunn's test highlighted significant differences

341 between most of the samples, except for the C1b which contained only 16 individuals (Table

342 2).

343

344 **Discussion**

345 *Reproductive anatomy*

346 The reproductive anatomy of *Protolira valvatoides* and *Pseudorimula midatlantica* showed

347 some differences leading to distinct reproductive attributes. *Protolira valvatoides* is a

348   simultaneous hermaphroditic gastropod with separated ovary and testis, characterized by the

349   presence of a propodial penis (Warén and Bouchet 1993) and internal fertilization as most of

350   the Skeneidae species (Haszprunar et al. 2016). Internal or pseudo-internal (i.e. entaquatic)

351   fertilization is an advantageous strategy adopted by many vent species that could ensure a

352   high level of fertilization by preventing the rapid dilution of gametes in the turbulent flow

353   regime of vents (Fretter 1989, Tyler and Young 1994, Hilario et al. 2005). Conversely,

354   *Pseudorimula midatlantica* is a gonochoric species with a large ovary occupying almost a third

355   of the body size. Unlike other genera of the Lepetodrilidae family (e.g. *Clypeosectus*,

356   *Gorgoleptis* and *Lepetodrilus*), *Pseudorimula* lack secondary reproductive organs such as a

357   penis or seminal groove (Haszprunar 1989; Warèn and Bouchet 2001) and no vesicle

358   containing sperm or fertilized oocytes have been found in females of this study. However,

359   Haszprunar (1989) identified the presence of ripe spermatozoa in contact with mucous

360   droplets of the prostate gland in *Pseudorimula marianae* males, suggesting an entaquatic

361   fertilization occurring after copulation in the female mantle cavities when oocytes are

362   released in the sea water. While the two species analysed in this study are known to be

363   associated with *Bathymodiolus azoricus* in cold habitats (Sarrazin et al. 2015), warmer fluid

364   zones can be as close as few to tens of centimetres (Sarrazin et al. 2014; Matabos et al. 2015).

365   Gametes released in seawater could thus easily be exposed to temperature above 100°C.

366   Some deep-sea gastropods are known to enclose embryos within egg capsules or gelatinous

367   mucus to protect them from harsh conditions (Berg 1985; Gustafson et al. 1991; Bouchet and

368   Warén 1991; Warén and Bouchet 2001; Martell et al. 2002; Watanabe et al. 2009), but to our

369   knowledge, none of the species belonging to the two investigated families display this type of

370   development.

371

372   *Gametogenesis*

373   The two species investigated displayed a similar gametogenic pattern with the presence of all

374   stages of oocyte development. The small oogonia of around 20 μm develop from the germinal

375   epithelium and evolve to previtellogenic oocytes. These previtellogenic oocytes reach 80-100

376   μm for *P. valvatoides* and 40-50 μm for *P. midatlantica,* after which they undergo

377   vitellogenesis, with a mean size of 185 μm for *P. valvatoides* and 81 μm for *P. midatlantica*.

378   The polymodal distribution and the absence of temporal variation of oocyte-size frequency

379   identified in this study for both species suggest iteroparity with a quasi-continuous and

380   asynchronous gametogenesis among individuals. These reproductive patterns have been

381   observed in many vent gastropod families such as Lepetodrilidae (Kelly and Metaxas 2007;

382   Tyler et al. 2008, Bayer et al. 2011; Nakamura et al. 2014), Peltospiridae (Fretter 1988;

383   Matabos and Thiebaut 2010) and Sutilizonidae (Hazsprunar 1989; Gustafson and Lutz, 1994).

384   Continuous or quasi-continuous gametogenesis is also found in other vent taxa, including

385   polychaetes (e.g. Alvinellidae, Ampharetidae, Polynoidae, and Siboglinidae families; McHugh

386   and Tunnicliffe 1994; McHugh 1995; Zal et al. 1995; Van Dover et al. 1999; Jollivet et al. 2000;

387   Blake and Van Dover 2005), shrimps (e.g. *Rimicaris chacei*, *Mirocaris fortunata*; Ramirez-

388   Llodra et al. 2000) and amphipods (*Halice hesmonectes, Bouvierella curtirama*; Sheader et al.

389   2000; 2004). This continuity in gametogenesis may be linked to the continuous supply of

390   energy in the vent environment, introduced in the food web by chemoautotrophic

391   microorganisms (Tyler et al. 1994). Thus, invertebrate species can allocate a constant supply

392   of energy for egg production and enhance the number of offspring throughout the year.

393   However, despite the absence of energy limitation, some vent species such as *Bathymodiolus*

394   *azoricus* display a seasonal reproduction with an annual emission of gametes around January

395   (Colaço et al. 2006; Dixon et al. 2006). Their periodic spawning and fertilisation events and

396   development of embryos into planktotrophic larvae seem to be linked to the seasonal input

397   of phytoplankton detritus from the surface sinking through the water column to the seafloor

398   (Gage and Tyler, 1991; Eckelbarger and Watling, 1995).

399

400   *Reproductive output*

401   The maximum oocyte-size found in *P. midatlantica* (176 μm) fell in the range of sizes

402   previously observed in the Lepetodrilidae family. Oocytes are larger than those of *Lepetodrilus*

403   *atlanticus, L. elevatus* and *L. ovalis*, but in the same order of magnitude as those of *L. fucensis*,

404   *L. cristatus*, *L. pustulosus* and *L. tevnianus* (Fretter 1988, Kelly and Metaxas 2007; Tyler et al.

405   2008; Matabos and Thiebaut 2010; Bayer et al. 2011). Oocyte size is commonly used as an

406   indicator of larval development mode. This assumes that large oocytes accumulate more yolk

407   and can provide enough energetic resources for a lecithotrophic nutrition when the larvae

408   disperse in the water column feeding only on the reserves accumulated in the eggs. On the

409   contrary, smaller eggs do not contain enough food reserves to support dispersing larvae, and

410   thus these larvae are mostly planktotrophic, feeding on bacteria, phytoplankton or detritus in

411   the water-column (Tyler 1988). The maximum egg size of 176 μm for *Pseudorimula*

412 *midatlantica* suggests a planktotrophic development for this species (Jaekle 1995; Levin and

413 Bridges 1995). However, for lepetodrilid species egg size appears to be a poor indicator of

414 larval development (Tyler et al. 2008). For instance, even if all lepetodrilid species studied to

415 date display quite small maximum oocytes size (<200 µm, Table 3), the morphology of their

416 larval shell is consistent with a lecitothrophic development (Tyler et al. 2008, Lutz et al. 1986).

417 This trait was proposed to reflect a phylogenetic constraint on vent taxa (Lutz et al. 1984). In

418 general, larvae that are dependent on the energy from the yolk have a limited dispersion

419 ability compared to planktotrophic larvae (Levin 2006). However, it has been demonstrated

420 that for deep-sea species, cold temperatures can lead to a reduction of the metabolism and a

421 delay of metamorphosis. This would enhance planktonic larval duration (PLD), suggesting the

422 potential for a wider dispersal range (Pradillon et al. 2001; Young 2003, Watanabe et al. 2006;

423 Adams et al. 2012).

424

425 When analysing the spatial variation of mean oocyte size and individual maturity for *P.*

426 *midatlantica* within LS vent field, we observed differences at the edifice scale, with larger

427 oocytes and higher proportion of mature oocytes in individuals of the C2a and R1 sites and

428 lower values in the C1a sample. In C1a, there was only one female among the 10 examined

429 individuals that could account for the observed difference in mean oocyte size compared to

430 other samples. Interestingly, the C2a and R1 locations displayed the warmer and more

431 variable temperatures, with mean temperature of 6.6 $\pm$ 0.9 °C for C2a and 8.3 $\pm$ 1.1 °C for

432 R1 compared to 5.7 ± 0.26 in C1a. The same observation was reported by Kelly and Metaxas

433 (2007) between active and senescent habitats for *L. fucensis* in the Juan de Fuca Ridge. These

434 authors showed poorly developed oocytes and lower fecundity in species inhabiting senescent

435 environments, suggesting an influence of habitat characteristics on reproductive outputs (i.e.

436 fecundity and oocyte size). Indeed, the proximity of vent emissions of warmer habitats might

437 enhance chemoautotrophic production (Guezennec et al. 1998, Sievert et al., 2000) and

438 provide a greater food supply for gastropods, allowing individuals to allocate more energy in

439 vitellogenesis.

440

441 Female fecundity and shell size showed a strong linear relationship in *P. midatlantica.* The

442 size-dependence of fecundity is a characteristic among many invertebrates, since larger

443 females are able to enhance their resource acquisition and allocate them to reproductive

444   processes (Bridges et al. 1994; Ramirez-Llodra 2002). This can also be supported by a positive

445   correlation between body size and the volume of the ovary that may contain more oocytes

446   (Honkoop and Van der Meer 1997). The maximum instantaneous fecundity of *P. midatlantica*

447   was 327 oocytes, measured in an individual of 8 mm. The lower fecundity of *P. midatlantica*

448   compared to other species of Lepetodrilid (Table 3) can be a result of the difference observed

449   in oocyte size: as this species has larger oocytes, less of them can be stored in the ovary.

450

451   *P. valvatoides* displayed an extremely low fecundity, with a maximum of 8 oocytes and no

452   relationship between fecundity and body size was observed. The specific trade-off between

453   size and number of mature oocytes due to individual body-size constraints can explain the low

454   fecundity observed in this species. The very small body size of *P. valvatoides* (below 4 mm) is

455   a common characteristic of Skeneidae species. However, *P. valvatoides* have large and yolky

456   vitellogenic oocytes with a maximum size of 272 μm, suggesting a lecithotrophic development

457   of the larvae (Haszprunar et al. 2016), similar to most vent gastropods (Lutz et al. 1984; Berg

458   1985; Gustafson and Lutz 1994). While the low fecundity observed in *P. valvatoides* may result

459   in a very weak probability to disperse at large scale and reach a new habitat, this species

460   remains very abundant within vent communities. The simultaneous hermaphroditism

461   observed in this species might contribute to maximizing the number of fertilized individuals,

462   resulting in a larger effective population size (i.e. number of individuals contributing to the

463   next generation). Hence, a large number of reproducing individuals could counteract the low

464   fecundity observed in *P. valvatoides* by ensuring a high retention rate and increasing the

465   number of larvae available for dispersal. This hypothesis requires further investigation and

466   population genetics approaches would bring additional insights in the dispersal of this species.

467

468   *Recruitment and population structure*

469   The polymodal size-frequency distribution observed within the different samples for both

470   species suggest episodic recruitment events. The discrepancy between continuous

471   gametogenesis and discontinuous recruitment has been previously observed in vent

472   gastropods (Matabos and Thiebaut 2010) and can be related to the occurrence of discrete

473   spawning events and/or post-settlement processes, including mortality and differential

474   growth. In addition, the number of juveniles found in this study is low and many factors can

475   explain this observation. First, the observed fecundity of the two species studied is low, thus

16

476 each spawning event would supply a small number of larvae, resulting in the settlement of
477 only a few specimens. Secondly, biotic and abiotic factors like competition for space or
478 physical stress on post-settled individuals may play a major role on mortality rates (Kelly and
479 Metaxas 2007). The observed differences in population structure among sampling locations
480 suggest variations in recruitment between different microhabitats, or could be linked to
481 differential mortality and growth rates specific to the habitat. This may be driven by spatial
482 variations in hydrothermal fluid flux, habitat heterogeneity or linked to differences in local
483 diversity that can, in turn, influence biotic interactions. Despite the extremely low fecundity
484 of *P. valvatoides*, the adult population present a high abundance of individuals that can reach
485 up to 4000 individuals.m^{-2} (Husson et al. 2017) in the different locations. Many hypotheses
486 can support this observation. On one hand, the combination of high density of organisms and
487 hermaphroditism might ensure the release of enough fertilized eggs to sustain the local
488 population. On the other hand, it could be possible that the emitted eggs are non-buoyant or
489 directly lay on hard substratum, as observed in other vent gastropods (Gustafson et al. 1991;
490 Fretter and Graham 1994; Yahagi et al. 2017). The direct development of this species within
491 the parental community would result in a high rate of retention within the community. In fact,
492 we noticed the presence of eggs laying on the sulphide substratum among faunal
493 assemblages, which could belong to *P. valvatoides*. Population genetic studies are necessary
494 to better understand the dispersal abilities for this species and determine the level of
495 population retention at the site scale.
496
497 *Implications for the resilience of vent communities*
498 A major disturbance at active hydrothermal vents, for example during deep-sea mining
499 operations, would lead to the collapse of the established faunal community. The first step in
500 the colonisation of newly formed low-temperature habitats is marked by the development of
501 free-living microbial communities (Shank et al. 1998). This large microbial production allows
502 the establishment of numerous metazoan species, among which, grazers and scavengers
503 represent the pioneer colonisers (Shank et al. 1998; Mullineaux et al. 2010; Mullineaux et al.
504 2012; Cuvelier et al. 2018). Then, the main pathway of macrofaunal recolonisation after a
505 large-scale disturbance is the settlement of larvae coming from adjacent areas (regional pool),
506 which results from the coincidence between the timing of disturbance and that of colonist
507 availabilities (Lutz et al. 1984; Pradillon et al. 2005, Mullineaux et al. 2010, 2012). Although

508 our knowledge regarding reproductive biology and dispersal capacity of vent species remains
509 scarce, some reproductive features of four dominant macrofaunal species of the Lucky Strike
510 vent field in the Mid-Atlantic Ridge have been investigated (Table 4). These species, which
511 include three gastropods (*L. atlanticus*, *P. midatlantica* and *P. valvatoides*) and the polychaete
512 *Amphisamytha lutzi,* are characterized by early maturity, quasi-continuous gametogenesis
513 and lecithotrophic larval development, which appears to be a common and widespread
514 successful reproductive strategy at vents. Continuous gametogenesis and lecithotrophic
515 development might ensure the continual presence of larvae in the environment and their
516 retention in the surrounding area.

517

518 Previous studies have hypothesized the implication of organic falls (e.g. whale falls) as
519 "stepping stones" that represent islands of food resources and suitable habitats for
520 chemosynthetically-fuelled species, and can thus play a connectivity role between vent and
521 seep habitats (Hecker 1985, Smith et al. 1989). *Protolira* species appear to be able to develop
522 on organic falls and feed on the local microbial production. Indeed, *Protolira thorvaldssoni* has
523 been found both at vent and seep environments, but also on whale bones, from which the
524 species was originally described (Waren 1996). *P. valvatoides* has also been recorded on wood
525 substrata deployed in inactive areas on the LS vent field (Alfaro-Lucas et al. in revision).
526 Despite their extremely low fecundity, *P. valvatoides* seems to be able to disperse as larvae,
527 and reach organic substrata, few hundred meters from active vents. This observation is not
528 consistent with our hypotheses of direct development of larvae and high retention rate for
529 this species, and many uncertainties remain regarding their dispersion. It is more likely that
530 the simultaneous hermaphroditism observed in this species represents an advantage over
531 gonochorism in situations in which finding a mate is difficult (Heller et al. 2008). Thus, even in
532 the case of low density of organisms on organic falls, *P. valvatoides* might ensure a relatively
533 good reproductive success and enhance their establishment by maximising the number of
534 offsprings.

535

536 To conclude, the two gastropod species considered in the present study exhibit some common
537 phylogenetically constrained reproductive traits, such as early maturity, quasi-continuous
538 gametogenesis and lecithotrophic larval development. This combination of reproductive traits
539 appears to be a widespread attribute among vent invertebrates to ensure the continuity of

540 larval supply and improve the sustainability of populations in the surrounding environment.
541 However, the two species showed contrasting reproductive features in terms of fecundity,
542 oocyte size and reproductive mode. Indeed, there is an important trade-off between the size
543 and the number of eggs produced by adults that is constrained by morphological and
544 physiological features and is highly dependent on energy availability. In this context, *P.*
545 *midatlantica* is characterized by the production of smaller mature oocytes counterbalanced
546 by a higher fecundity compared to *P. valvatoides*. This specific strategy may enhance
547 recruitment success by maximizing the number of offsprings but reduce the ability to disperse
548 further because less energy is allocated to a single oocyte. Conversely, *P. valvatoides* produces
549 a very low number of bigger oocytes. For this species, small adult size associated with reduced
550 ovary volume constrain the reproductive output. Despite its low fecundity, *P. valvatoides*
551 hermaphroditism may be an advantage to enhance the number of fertilized eggs and maintain
552 an important effective population size at the local scale. Therefore, in the context of major
553 disturbance, habitat destruction could lead to a collapse of local populations for both species.
554 Furthermore, despite differences in the reproductive characteristics of the two investigated
555 species, their ability to disperse widely from a preserved area and reach impacted sites seems
556 highly limited by their low fecundity and their dispersal mode (lecithotrophy). However,
557 previous results suggest that *P. valvatoides* might be able to use organic falls as stepping
558 stones to disperse and recolonize an impacted area.

559

560 Finally, this study provides new data on key biological features that can feed bio-physical
561 models of connectivity. In addition, it highlighted that the description of reproductive biology
562 is not sufficient to comprehend all the mechanisms involved in the dispersion and
563 establishment of vent species. Indeed, the role of environmental factors, particularly ocean
564 currents and water column food supply, are essential factors to ensure the settlement of
565 dispersing larvae in newly formed habitats. Therefore, knowledge of biological features and
566 environmental factors associated with population genetics/genomics approaches are needed
567 to better understand the dispersal potential of species inhabiting chemosynthetic-based
568 ecosystems, and the resilience of vent communities (Hilario et al., 2015; Baco et al., 2016).
569 This knowledge is fundamental to define restoration actions that might be implemented to
570 ensure ecosystem sustainability in case of large-scale disturbances induced by mining
571 activities. Thus, the establishment of efficient protected areas with buffer zones and the

deployment of artificial substrata that can act as stepping stones for vent species to recolonize impacted areas, represent important measures to take into consideration.

Compliance with Ethical Standards

Conflicts of interest The authors declare that they have no conflict of interest.

Ethics approval All applicable international, national, and/or institutional guidelines for sampling were followed in the current study.

Consent to participate Not applicable

600 **Consent for publication** The Author hereby consents to publication of the work in any and
601 all Springer publications. The Author warrants that the work has not been published in any
602 form except as a preprint that the work is not being concurrently submitted to and is not
603 under consideration by another publisher.

604 **Availability of data and material** Not applicable

605 **Code availability** Not applicable

606 **Authors' contributions** JM, MM, JS and ERLL conceived the ideas and designed the
607 methodology. JM, MM and JS collected the data and JM processed and analysed the data.
608 JM wrote the first draft of the manuscript and all authors commented on previous versions
609 of the manuscript. All authors read and approved the final manuscript.

610 **Tables**

611 **Table 1**. Summary of vent sites and stations, time of sampling, number of individuals and
612 shell size range of all individuals of the two species used for histological analyses in this
613 study. Mean and standard deviation of temperature measured on each quadrat during a
614 year are also presented.

Species	Edifice	Station	Date	Number of individuals	Shell length range (mm)	Temperature (°C) (mean ± sd)
Prototolira valvatoides	Montségur	C1a	July 2017	5	1.7–2.6	5.7 ± 0.26
			August 2018	5	1.9–2.7	
		C1acg	July 2017	4	1.9–2.8	5.1 ± 0.08
			August 2018	12	1.8–3.1	
		C1bcg	August 2018	7	1.9–2.6	5.3 ± 0.38
		C2a	July 2017	3	1.7–2.7	6.6 ± 0.92
		R1	August 2018	4	1.8–2.9	8.3 ± 1.13
	Eiffel Tower	ET	April 2015	18	1.8–3.5	5.3 ± 0.36
Pseudorimula midatlantica	Montségur	C1a	July 2017	1	4.7	5.7 ± 0.26
		C1acg	August 2018	10	4–6.5	5.1 ± 0.08
		C1b	August 2018	3	3.6–5	5.1 ± 0.3
		C1bcg	August 2018	5	3.3–5.7	5.3 ± 0.38
		C2a	July 2017	5	4.2–5.9	6.6 ± 0.92
		C2bcg	July 2017	2	4.6–5.3	5.3 ± 0.42
		R1	July 2018	3	3.9–6.7	8.3 ± 1.13
	Eiffel Tower	ET	April 2015	5	4.1–5.8	5.3 ± 0.36

615

616 **Table 2**. Matrix of p-value of the Nemenyi and Dunn multiple range test used to compare the

617 shell length distribution of *Protolira valvatoides* (up-right) and *Pseudorimula midatlantica*

618 (down-left) among the different locations. ns = not significant ; *p<0.05; **p<0.01;

619   ***p<0.001.

Quadrat	C1a	C1acg	C1b	C1bcg	C2a	C2bcg	R1
C1a		***	.	*	**	.	*
C1acg	***		.	***	ns	.	ns
C1b	***	ns		.	.	.	.
C1bcg	*	***	*		***	.	**
C2a	***	**	ns	***		.	*
C2bcg	**	*	ns	ns	***		.
R1	***	ns	ns	***	***	***	

620

Table 3. Summary of known reproductive traits of hydrothermal vent limpets from the

Lepetodrilidae family. JDFR: Juan de Fuca Ridge, EPR: East Pacific Rise, MAR: Mid-Atlantic

Ridge.

Species	Date	Location	Maximum size of vitellogenic oocytes (µm)	Onset of vitellogenesis (µm)	Instantaneous fecundity (Mean ± SD) [Max]	References
Lepetodrilus fucensis	Jul. 2001	JFDR	110	35-45	125.7 ± 121.4 [5149]	Kelly and Metaxas (2007)
	Jul.–Sept. 1984		140			Fretter (1988)
Lepetodrilus pustulosus	Mar. 1984	EPR	120			Fretter (1988)
	Dec. 2001		84	30–35	53.9 ± 42.3 [850]	Pendlebury (2005); Tyler et al. (2008)
	Apr.–May 1979		104			Berg (1985)
Lepetodrilus elevatus	Dec. 2001	EPR	84	30–35	[1800]	Pendlebury (2005); Tyler et al. (2008)
	Apr.–May 1979		95			Berg (1985)
Lepetodrilus. ovalis	Dec. 2001	EPR	87	30–35	27.9 ± 32.6 [400]	Pendlebury (2005); Tyler et al. (2008)
Lepetodrilus. cristatus	Mar.1984	EPR	150	30–35		Fretter (1988)
Lepetodrilus tevnianus	Dec.2006	EPR	210	35–40		Bayer et al. (2011)
Lepetodrilus atlanticus	Mar.–Apr. 2001	MAR	92	35–40	37.2 ± 24.1 [300]	Pendlebury (2005); Tyler et al. (2008)
seudorimula. midatlantica	Apr. 2015	MAR	155	40-50	187 ± 44 [327]	This study
	Jul. 2017		175			This study
	Aug. 2018		176			This study

625   **Table 4**. Summary of known reproductive traits of dominant species of the Lucky Strike vent

626   field. *Fecundity refers to the total number of oocytes within a female regardless of the

627   development stage while it refers to the number of vitellogenic oocytes for the other studies.

Species	Reproductive strategy	Size of vitellogenic oocytes (µm)	Fecundity	Larval devlopment	Seasonality	References
Bathymodiolus azoricus	Gonochoric	70-80	No data	Planktotrophic	Seasonal	Colaço et al. (2006) Dixon et al. (2006)
Branchipolynoe seepensis	Gonochoric	250-500	100-300	Lecithotrophic	Quasi-continuous	Jollivet et al. (2006)
Amphisamytha lutzi	Gonochoric	150-190	> 2500 *	Lecithotrophic	Quasi-continuous	Blake et al. (2005)
Lepetodrillus atlanticus	Gonochoric	50 - 92	95-300	Lecithotrophic	Quasi-continuous	Tyler et al. (2008)
Pseudorimula midatlantica	Gonochoric	80 - 176	107- 327	Lecithotrophic	Quasi-continuous	This study
Protolira valvatoides	Hermaphrodite	120 - 272	4 - 8	Lecithotrophic	Quasi-continuous	This study

628

629   **Figure legends**

630

631   **Fig.1** A. Location of the Lucky Strike vent field on the Mid-Atlantic ridge, south of the Azores.

632   B. The 1 km^2 LS vent field with the Montségur and Eiffel Tower edifices on the south-east. C.

633   Location of the different sampling locations on and around the Montségur edifice.

634

635   **Fig.2** Morphology of reproductive structures of *Protolira valvatoides* (left) and *Pseudorimula*

636   *midatlantica* (right). **A**. Dorsal view of *P. valvatoides* soft body. **B**. Ventral view of *P.*

637   *midatlantica* soft body. **C**. General view of a transversal section of *P. valvatoides.* **D**. General

638   view of a transversal section of a *P. midatlantica* female. **E.** Detailed view of *P. valvatoides*

639   ovary. **F**. Detailed view of *P. midatlantica* ovary. **G.** Detailed of *P. valvatoides* testis. **H.** Detailed

640   view of *P. midatlantica* testis. Abbreviations: *ct: ctenidium; dg: digestive glands; f: foot, ov:*

641   *ovary; oo: oogonia; pvo: previtellogenic oocyte; s: snout; st: stomach; spd: spermatid; spg:*

642   *spermatogonia; spz: spermatozoa; t: testis; vo: vitellogenic oocytes. Scale bars: A and C= 1mm;*

643   *B and D= 2mm; E, F and H= 200 µm; G= 50 µm.*

644

645   **Fig.3** Mean oocyte size-frequency histograms (mean ± SD) of pooled individuals of *Protolira*

646   *valvatoides* for each quadrat. Colors: Grey bars represent previtellogenic oocytes and yellow

647   bars represent vitellogenic oocytes. Abbreviations: *N*, number of individuals; *n*, number of

648   oocytes measured.

649

Fig.4 Mean oocyte size-frequency histograms (mean ± SD) of pooled individuals of *Pseudorimula midatlantica* for each quadrat. Colors: Grey bars represent previtellogenic oocytes and yellow bars represent vitellogenic oocytes. Abbreviations: *N*, number of individuals; *n*, number of oocytes measured.

Fig.5 Box-plot of the oocyte size-distribution of the two studied gastropods *Protolira valvatoides* (left) and *Pseudorimula midatlantica* (right) among the different samples. The mean oocyte size is represented by a black diamond **A**. Boxplot showing the oocyte-size distribution of each individual of *P. valvatoides* among the different samples. **B**. Boxplot showing the oocyte-size distribution of each individual of *P. midatlantica* among the different samples. **C**. Boxplot showing the oocyte-size distribution of pooled individuals of *P. valvatoides* among the different samples. **D**. Boxplot showing the oocyte-size distribution of pooled individuals of *P. midatlantica* among the different samples. Abbreviations: *N*, number of individuals; *n*, number of oocytes measured. Multisample comparisons were performed using the Nemenyi and Dunn test; homogeneous groups share the same letter.

Fig.6 Relationship between animal shell length and proportion of vitellogenic oocytes for each specimen of **A**. *Protolira valvatoides* and **B**. *Pseudorimula midatlantica* among the different samples.

Fig.7 Size-frequency distribution of shell length of **A**. *Protolira valvatoides* and **B**. *Pseudorimula midatlantica* among the different samples. Abbreviations: *n*, number of individuals measured.

677 **Supplementary material**

678 **Table S1**. Results of Kruskal–Wallis multisample tests and the Nemenyi and Dunn multiple

679 range tests comparing oocyte size distributions between individuals of the two gastropod

680 species within each sample.

Species	Edifice	Station	Date	Number of individuals	Kruskal-Wallis multisample test	Nemenyi and Dunn multiple range test
Prototolira valvatoides	Montségur	C1a	July 2017	5	H = 29.69, df = 4, P < 0.001	1/5 different
			August 2018	5	H = 7.87, df = 4, P < 0.05	2/5 different
		C1acg	July 2017	4	H = 6.25, df = 3, P < 0.05	1/4 different
			August 2018	12	H = 153.72, df = 11, P < 0.001	3/12 different
		C1bcg	August 2018	7	H = 70.49, df = 6, P < 0.001	2/7 different
		C2a	July 2017	3	H = 1.23, df = 2, P > 0.05	-
		R1	August 2018	4	H = 13.12, df = 4, P < 0.05	1/4 different
	Eiffel Tower	ET	April 2015	18	H = 107.51, df = 17, P < 0.001	2/18 different
Pseudorimula midatlantica	Montséegur	C1a	July 2017	1	-	-
		C1acg	August 2018	10	H = 23.54, df = 9, P < 0.05	2/10 different
		C1b	August 2018	3	H = 1.89, df = 2, P > 0.05	-
		C1bcg	August 2018	5	H = 8.66, df = 4, P > 0.05	-
		C2a	July 2017	5	H = 10.47, df = 4, P < 0.01	1/5 different
		C2bcg	July 2017	2	H = 8.22, df = 1, P < 0.05	1/2 different
		R1	July 2017	3	H = 63.06, df = 2, P < 0.001	1/3 different
	Eiffel Tower	ET	April 2015	5	H = 40.10, df = 4, P < 0.001	2/5 different

681

682 **Fig.S1** Mean oocyte size-frequency histograms (mean ± SD) of pooled individuals of *Protolira*

683 *valvatoides* for each sampling period. Colors: Grey bars represent previtellogenic oocytes and

684 yellow bars represent vitellogenic oocytes. Abbreviations: *N*, number of individuals; *n*, number

685 of oocytes measured.

686 **Fig.S2** Mean oocyte size-frequency histograms (mean ± SD) of pooled individuals of

687 *Pseudorimula midatlantica* for each sampling period. Colors: Grey bars represent

688 previtellogenic oocytes and yellow bars represent vitellogenic oocytes. Abbreviations: *N*,

689 number of individuals; *n*, number of oocytes measured.

690

691 **DOI of the cruises involved**

692 SARRADIN Pierre-Marie, CANNAT Mathilde (2015) MOMARSAT2015 cruise, RV Pourquoi pas

693 ?, https://doi.org/10.17600/15000200

694 SARRADIN Pierre-Marie, CANNAT Mathilde (2017) MOMARSAT2017 cruise, RV Pourquoi pas
695 ?, https://doi.org/10.17600/17000500

696 CANNAT Mathilde (2018) MOMARSAT2018 cruise, RV L'Atalante,
697 https://doi.org/10.17600/18000514

698 **References**

699 Adams, D.K., S.M. Arellano, and B. Govenar. (2012). Larval dispersal: Vent life in the water
700   column. Oceanography 25(1): 256–268. doi: 10.5670/oceanog.2012.24.

701 Baco AR, Etter RJ, Ribeiro PA, Heyden S von der, Beerli P, Kinlan BP (2016) A synthesis of
702   genetic connectivity in deep-sea fauna and implications for marine reserve design. Mol
703   Ecol 25: 3276–3298. doi: 10.1111/mec.13689

704 Bates AE (2006) Population and feeding characteristics of hydrothermal vent gastropods
705   along environmental gradients with a focus on bacterial symbiosis hosted by
706   *Lepetodrilus fucensis* (Vetigastropoda). PhD Thesis
707 Bayer SR, Mullineaux LS, Waller RG, Solow AR (2011) Reproductive traits of pioneer
708   gastropod species colonizing deep-sea hydrothermal vents after an eruption. Mar Biol
709   158: 181–192. doi: 10.1007/s00227-010-1550-1
710 Blake EA, Dover CLV (2005) The reproductive biology of Amathys lutzi, an ampharetid
711   polychaete from hydrothermal vents on the Mid-Atlantic Ridge. Invertebr Biol 124: 254–
712   264. doi: 10.1111/j.1744-7410.2005.00022.x
713 Berg, C. J. (1985) Reproductive strategies of mollusks from abyssal hydrothermal vent
714   communities. Bull Biol Soc Wash 6: 185-197
715 Boschen RE, Rowden AA, Clark MR, Pallentin A, Gardner JPA (2016) Seafloor massive sulfide
716   deposits support unique megafaunal assemblages: Implications for seabed mining and
717   conservation. Mar Environ Res 115: 78–88. doi: 10.1016/j.marenvres.2016.02.005
718 Bouchet, P. and Warén, A. (1991) *Ifremeria nautilei,* a new gastropod from hydrothermal
719   vents, probably associated with symbiotic bacteria. Cr Acad Sci Iii-Vie 312, 495–501.
720 Breusing C, Biastoch A, Drews A, Metaxas A, Jollivet D, Vrijenhoek RC, Bayer T, Melzner F,
721   Sayavedra L, Petersen JM, Dubilier N, Schilhabel MB, Rosenstiel P, Reusch TBH (2016)
722   Biophysical and Population Genetic Models Predict the Presence of "Phantom" Stepping
723   Stones Connecting Mid-Atlantic Ridge Vent Ecosystems. Curr Biol 26: 2257–2267. doi:
724   10.1016/j.cub.2016.06.062
725 Bridges TS, Levin LA, Cabrera D, Plaia G (1994) Effects of sediment amended with sewage,
726   algae, or hydrocarbons on growth and reproduction in two opportunistic polychaetes. J
727   Exp Mar Biol Ecol 177: 99–119. doi: 10.1016/0022-0981(94)90146-5
728 Carpenter S, Walker B, Anderies JM, Abel N (2001) From Metaphor to Measurement:
729   Resilience of What to What? Ecosystems 4:765–781. doi: 10.1007/s10021-001-0045-9
730 Clark, M.R., Smith, S., (2013) Environ Manag Consid. In: Deep Sea Minerals: Manganese
731   Nodules, A Physical, Biological, Environmental and Technical Review, SPC1B, pp. 27e41
732 Colaço A, Martins I, Laranjo M, Pires L, Leal C, Prieto C, Costa V, Lopes H, Rosa D, Dando PR,
733   Serrão-Santos R (2006) Annual spawning of the hydrothermal vent mussel,
734   *Bathymodiolus azoricus*, under controlled aquarium, conditions at atmospheric
735   pressure. J Exp Mar Biol Ecol 333: 166–171. doi: 10.1016/j.jembe.2005.12.005

736 Colaço A, Desbruyères D, Guezennec J (2007) Polar lipid fatty acids as indicators of trophic
737   associations in a deep-sea vent system community. Mar Ecol 28: 15–24. doi:
738   10.1111/j.1439-0485.2006.00123.x
739 Connell SD, Ghedini G (2015) Resisting regime-shifts: the stabilising effect of compensatory
740   processes. Trends Ecol Evol 30: 513–515. doi: 10.1016/j.tree.2015.06.014
741 Cumming GS, Olsson P, Chapin FS, Holling CS (2013) Resilience, experimentation, and scale
742   mismatches in social-ecological landscapes. Landscape Ecol 28: 1139–1150. doi:
743   10.1007/s10980-012-9725-4
744 Cuvelier D, Beesau J, Ivanenko VN, Zeppilli D, Sarradin P-M, Sarrazin J (2014) First insights
745   into macro- and meiofaunal colonisation patterns on paired wood/slate substrata at
746   Atlantic deep-sea hydrothermal vents. Deep-Sea Res Pt I 87: 70–81. doi:
747   10.1016/j.dsr.2014.02.008
748 Cuvelier D, Gollner S, Jones DOB, Kaiser S, Arbizu PM, Menzel L, Mestre NC, Morato T, Pham
749   C, Pradillon F, Purser A, Raschka U, Sarrazin J, Simon-Lledó E, Stewart IM, Stuckas H,
750   Sweetman AK, Colaço A (2018) Potential Mitigation and Restoration Actions in
751   Ecosystems Impacted by Seabed Mining. Front Mar Sci. doi: 10.3389/fmars.2018.00467
752 De Busserolles F, Sarrazin J, Gauthier O, Gélinas Y, Fabri MC, Sarradin PM, Desbruyères D
753   (2009) Are spatial variations in the diets of hydrothermal fauna linked to local
754   environmental conditions? Deep-Sea Res Pt II 56:1649–1664. doi:
755   10.1016/j.dsr2.2009.05.011
756 DeFreese DE, Clark KB (1983) Analysis of reproductive energetics of Florida Opisthobranchia
757   (Mollusca: Gastropoda). Int J Inver Rep 6: 1–10. doi: 10.1080/01651269.1983.10510018
758 Desbruyères D, Biscoito M, Caprais J-C, Colaço A, Comtet T, Crassous P, Fouquet Y,
759   Khripounoff A, Le Bris N, Olu K, Riso R, Sarradin P-M, Segonzac M, Vangriesheim A
760   (2001) Variations in deep-sea hydrothermal vent communities on the Mid-Atlantic Ridge
761   near the Azores plateau. Deep-Sea Res Pt I 48: 1325–1346. doi: 10.1016/S0967-
762   0637(00)00083-2
763 Desbruyères D, Segonzac M, Bright M, Biologiezentrum OL, Desbruyeres D, Segonzac M,
764   Bright M (2006) Handbook of deep-sea hydrothermal vent fauna, 2nd completely rev.
765   ed. / editors, Daniel Desbruyères, Michel Segonzac and Monika Bright. Linz, Austria :
766   Land Oberösterreich, Biologiezentrum der Oberösterreichische Landesmuseen
767 Dixon DR, Lowe DM, Miller PI, Villemin GR, Colaço A, Serrão-Santos R, Dixon LRJ (2006)
768   Evidence of seasonal reproduction in the Atlantic vent mussel *Bathymodiolus azoricus*,
769   and an apparent link with the timing of photosynthetic primary production. J of the J
770   Mar Biol Assoc UK 86: 1363–1371. doi: 10.1017/S0025315406014391
771 Eckelbarger KJ, Eckelbarger KJ (1994) Diversity Of Metazoan Ovaries And Vitellogenic
772   Mechanisms - Implications For Life history Theory. P Biol Soc Wash 107: 193–218.
773 Eckelbarger KJ, Watling L (1995) Role of Phylogenetic Constraints in Determining
774   Reproductive Patterns in Deep-Sea Invertebrates. Inver Biol 114:256–269. doi:
775   10.2307/3226880
776 Fretter V (1988) New archaeogastropod limpets from hydrothermal vents; Superfamily
777   Lepetodrilacea. II. Anatomy. Philos T Roy Soc B 319:33–82. doi: 10.1098/rstb.1988.0032
778 Fretter V (1989) The anatomy of some new archaeogastropod limpets (Superfamily
779   Peltospiracea) from hydrothermal vents. J Zool 218: 123–169. doi: 10.1111/j.1469-
780   7998.1989.tb02530.x
781 Fretter V, Graham A (1994) British prosobranch molluscs. Their functional anatomy and
782   ecology. Publ Brit Ray Soc, No. 144

783   Gabe M (1968) Techniques histologiques. Masson

784   Gage JD, Tyler PA (1991) Deep-Sea Biology: A Natural History of Organisms at the Deep-Sea
785   Floor. Camb U Pr

786   Galkin SV, Goroslavskaya EI (2010) Bottom fauna associated with *Bathymodiolus azoricus*
787   (Mytilidae) mussel beds in the hydrothermal fields of the Mid-Atlantic Ridge.
788   Oceanology 50: 51–60. doi: 10.1134/S0001437010010066

789   Gladstone-Gallagher RV, Pilditch CA, Stephenson F, Thrush SF (2019) Linking Traits across
790   Ecological Scales Determines Functional Resilience. Trends Ecol Evol 34: 1080–1091. doi:
791   10.1016/j.tree.2019.07.010

792   Gollner S, Govenar B, Arbizu PM, Mills S, Le Bris N, Weinbauer M, Shank TM, Bright M (2015)
793   Differences in recovery between deep-sea hydrothermal vent and vent-proximate
794   communities after a volcanic eruption. Deep-Sea Res Pt I 106: 167–182. doi:
795   10.1016/j.dsr.2015.10.008

796   Gollner S, Kaiser S, Menzel L, Jones DOB, Brown A, Mestre NC, van Oevelen D, Menot L,
797   Colaço A, Canals M, Cuvelier D, Durden JM, Gebruk A, Egho GA, Haeckel M, Marcon Y,
798   Mevenkamp L, Morato T, Pham CK, Purser A, Sanchez-Vidal A, Vanreusel A, Vink A,
799   Martinez Arbizu P (2017) Resilience of benthic deep-sea fauna to mining activities. Mar
800   Environ Res 129:76–101. doi: 10.1016/j.marenvres.2017.04.010

801   Guezennec J, Ortega-Morales O, Raguenes G, Geesey G (1998) Bacterial colonization of
802   artificial substrate in the vicinity of deep-sea hydrothermal vents. FEMS Microbiol Ecol
803   26:89–99. doi: 10.1016/S0168-6496(98)00022-1

804   Gustafson RG, Littlewood DTJ, Lutz RA (1991) Gastropod Egg Capsules and Their Contents
805   From Deep-Sea Hydrothermal Vent Environments. Biol Bull 180: 34–55. doi:
806   10.2307/1542427

807   Gustafson RG and Lutz RA (1994). Molluscan life history traits at deep sea hydrothermal
808   vents and cold methane/ sulfide seeps. In Reproduction, larval biology, and recruitment
809   in deep-sea benthos (ed. C.M. Young and K. Eckelbarger), pp.76-97. NewYork: Columb U
810   Pr

811   Haszprunar G (1989) New slit-limpets (Scissurellacea and Fissurellacea) from hydrothermal
812   vents. Part 2. Anatomy and relationships. Contrib. sci. (Los Angel. Calif.) 408: 1-17.

813   Haszprunar G, Kunze T, Brückner M, Heß M (2016) Towards a sound definition of Skeneidae
814   (Mollusca, Vetigastropoda): 3D interactive anatomy of the type species, Skenea
815   serpuloides (Montagu, 1808) and comments on related taxa. Org Divers Evol 16:577–
816   595. doi: 10.1007/s13127-015-0260-4

817   Hecker B (1985) Fauna from a cold sulfur-seep in the Gulf of Mexico: comparison with
818   hydrothermal vent communities and evolutionary implications. Bull Biol Soc Wash 6:
819   465-473.

820   Hein JR, Mizell K, Koschinsky A, Conrad TA (2013) Deep-ocean mineral deposits as a source of
821   critical metals for high- and green-technology applications: Comparison with land-based
822   resources. Ore Geol Rev 51: 1–14. doi: 10.1016/j.oregeorev.2012.12.001

823   Heller J (1993) Hermaphroditism in molluscs. Biol J Linn Soc 48:19–42. doi: 10.1111/j.1095-
824   8312.1993.tb00874.x

825   Hilário A, Young CM, Tyler PA (2005) Sperm Storage, Internal Fertilization, and Embryonic
826   Dispersal in Vent and Seep Tubeworms (Polychaeta: Siboglinidae: Vestimentifera). Biol
827   Bull 208: 20–28. doi: 10.2307/3593097

828 Hilário A, Metaxas A, Gaudron SM, Howell KL, Mercier A, Mestre NC, Ross RE, Thurnherr AM,
829   Young C (2015) Estimating dispersal distance in the deep sea: challenges and
830   applications to marine reserves. Front Mar Sci. doi: 10.3389/fmars.2015.00006
831 Honkoop PJC and Van der Meer J (1997). Reproductive output of Macoma balthica
832   populations in relation to winter-temperature and intertidalheight mediated changes of
833   body mass. Mar Ecol Prog. Ser. 149, 155-162.
834 Husson B, Sarradin P-M, Zeppilli D, Sarrazin J (2017) Picturing thermal niches and biomass of
835   hydrothermal vent species. Deep-Sea Res Pt II 137: 6–25. doi:
836   10.1016/j.dsr2.2016.05.028
837 Ingrisch J, Bahn M (2018) Towards a Comparable Quantification of Resilience. Trends Ecol
838   Evol 33: 251–259. doi: 10.1016/j.tree.2018.01.013
839 Jaeckle W (1995) Variation in the Size, Energy Content, and Biochemical Composition of
840   Invertebrate Eggs: Correlates to the Mode of Larval Development. pp. 49 –77 in Ecol of
841   Mar Inver Larv, L. Mc Edward, ed. CRC Press, Boca Raton, FL
842 Jollivet D, Empis A, Baker MC, Hourdez S, Comtet T, Jouin-Toulmond C, Desbruyères D, Tyler
843   PA (2000) Reproductive biology, sexual dimorphism, and population structure of the
844   deep sea hydrothermal vent scale-worm, *Branchipolynoe seepensis* (Polychaeta:
845   Polynoidae). J Mar Biol Ass UK 80: 55–68. doi: 10.1017/S0025315499001563
846 Kelly NE, Metaxas A (2007) Influence of habitat on the reproductive biology of the deep-sea
847   hydrothermal vent limpet *Lepetodrilus fucensis* (Vetigastropoda: Mollusca) from the
848   Northeast Pacific. Mar Biol 151:649–662. doi: 10.1007/s00227-006-0505-z
849 Laming SR, Gaudron SM, Duperron S (2018) Lifecycle Ecology of Deep-Sea Chemosymbiotic
850   Mussels: A Review. Front Mar Sci. doi: 10.3389/fmars.2018.00282
851 Levin LA., Bridges TS. (1995) Pattern and diversity in reproduction and development. In:
852   McFdward LR, ed. Ecol Mar Inver Larv. Boca Raton, Florida: CRC Press, 1-48.
853 Levin LA (2006) Recent progress in understanding larval dispersal: new directions and
854   digressions. Integr Comp Biol 46: 282–297. doi: 10.1093/icb/icj024
855 Levin LA, Mengerink K, Gjerde KM, Rowden AA, Van Dover CL, Clark MR, Ramirez-Llodra E,
856   Currie B, Smith CR, Sato KN, Gallo N, Sweetman AK, Lily H, Armstrong CW, Brider J
857   (2016) Defining "serious harm" to the marine environment in the context of deep-
858   seabed mining. Mar Pol 74: 245–259. doi: 10.1016/j.marpol.2016.09.032
859 Lutz RA, Jablonski D, Turner RD (1984) Larval Development and Dispersal at Deep-Sea
860   Hydrothermal Vents. Science 226: 1451–1454. doi: 10.1126/science.226.4681.1451
861 Lutz RA, Bouchet P, Jablonski D, Turner RD, and Warén A (1986), Larval ecology of mollusks at
862   deep-sea hydrothermal vents, Am Malacol Bull 4, 49-54,
863 Mac Donald P, Du with contributions from J (2018) mixdist: Finite Mixture Distribution
864   Models.
865 Martell KA, Tunnicliffe V, Macdonald IR (2002) Biological features of a buccinid whelk
866   (Gastropoda, Neogastropoda) at the Endeavour Vent-field of Juand de Fuca Ridge,
867   Northest Pacific. J Molluscan Stud 68:45–53. doi: 10.1093/mollus/68.1.45
868 Matabos M, Thiebaut E (2010) Reproductive biology of three hydrothermal vent peltospirid
869   gastropods (*Nodopelta heminoda, N. subnoda* and *Peltospira operculata*) associated
870   with Pompeii worms on the East Pacific Rise. J Molluscan Stud 76:257–266. doi:
871   10.1093/mollus/eyq008
872 Matabos M, Cuvelier D, Brouard J, Shillito B, Ravaux J, Zbinden M, Barthelemy D, Sarradin
873   PM, Sarrazin J (2015) Behavioural study of two hydrothermal crustacean decapods:

Mirocaris fortunata and *Segonzacia mesatlantica*, from the Lucky Strike vent field (Mid-Atlantic Ridge). Deep-Sea Res Pt II 121: 146–158. doi: 10.1016/j.dsr2.2015.04.008

McHugh D (1995) Unusual Sperm Morphology in a Deep-Sea Hydrothermal-Vent Polychaete, *Paralvinella pandorae* (Alvinellidae). Inver Biol 114: 161–168. doi: 10.2307/3226888

McHugh D, Tunnicliffe V (1994) Ecology and reproductive biology of the hydrothermal vent polychaete *Amphisamytha galapagensis* (Ampharetidae). Mar Ecol Progr Ser 106:111–120. doi: 10.3354/meps106111

McLean JH, Haszprunar G (1987) Pyropeltidae, a new family of cocculiniform limpets from hydrothermal vents. Veliger 30:196–205

McLean JH (1992) A new species of Pseudorimula (Fissurellacea: Clypeosectidae) from hydrothermal vents of the Mid-Atlantic Ridge. Nautilus 106(3): 115-118

Metaxas A, Saunders M (2009) Quantifying the "Bio-" Components in Biophysical Models of Larval Transport in Marine Benthic Invertebrates: Advances and Pitfalls. Biol Bull 216: 257–272. doi: 10.1086/BBLv216n3p257

Mullineaux LS, Adams DK, Mills SW, Beaulieu SE (2010) Larvae from afar colonize deep-sea hydrothermal vents after a catastrophic eruption. PNAS 107:7829–7834. doi: 10.1073/pnas.0913187107

Mullineaux LS, Bris NL, Mills SW, Henri P, Bayer SR, Secrist RG, Siu N (2012) Detecting the Influence of Initial Pioneers on Succession at Deep-Sea Vents. PLOS ONE 7:e50015. doi: 10.1371/journal.pone.0050015

Nakamura M, Watanabe H, Sasaki T, Ishibashi J, Fujikura K, Mitarai S (2014) Life history traits of *Lepetodrilus nux* in the Okinawa Trough, based upon gametogenesis, shell size, and genetic variability. Mar Ecol Progr Ser 505:119–130. doi: 10.3354/meps10779

Oliver TH, Heard MS, Isaac NJB, Roy DB, Procter D, Eigenbrod F, Freckleton R, Hector A, Orme CDL, Petchey OL, Proença V, Raffaelli D, Suttle KB, Mace GM, Martín-López B, Woodcock BA, Bullock JM (2015) Biodiversity and Resilience of Ecosystem Functions. Trends Ecol Evol 30:673–684. doi: 10.1016/j.tree.2015.08.009

Portail M, Brandily C, Cathalot C, Colaço A, Gélinas Y, Husson B, Sarradin P-M, Sarrazin J (2018) Food-web complexity across hydrothermal vents on the Azores triple junction. Deep-Sea Res Pt I 131:101–120. doi: 10.1016/j.dsr.2017.11.010

Pradillon F, Shillito B, Young CM, Gaill F (2001) Developmental arrest in vent worm embryos. Nature 413:698–699. doi: 10.1038/35099674

Pradillon F, Bris NL, Shillito B, Young CM, Gaill F (2005) Influence of environmental conditions on early development of the hydrothermal vent polychaete *Alvinella pompejana*. J Exp Biol 208:1551–1561. doi: 10.1242/jeb.01567

Pendlebury S (2005) Ecology of hydrothermal vent gastropods. PhD thesis. School of Ocean and Eart Sciences, Southampton, 148 pp.

Ramirez-Llodra E (2002) Fecundity and life-history strategies in marine invertebrates. In: Adv Mar Biol pp 87–170

Ramirez-Llodra E, Tyler PA, Baker MC, Bergstad OA, Clark MR, Escobar E, Levin LA, Menot L, Rowden AA, Smith CR, Dover CLV (2011) Man and the Last Great Wilderness: Human Impact on the Deep Sea. PLOS ONE 6:e22588. doi: 10.1371/journal.pone.0022588

Ramirez-Llodra R, Tyler PA, Copley JTP (2000) Reproductive biology of three caridean shrimp, *Rimicaris exoculata, Chorocaris chacei* and *Mirocaris fortunata* (Caridea: Decapoda), from hydrothermal vents. J Mar Biol Ass U K 80:473–484. doi: 10.1017/S0025315400002174

920   R Studio Team (2016). RStudio: Integrated Development Environment for R. Boston, MA:
921   RStudio, Inc. Available at: http://www.rstudio.com
922   Sarrazin J, Cuvelier D, Peton L, Legendre P, Sarradin PM (2014) High-resolution dynamics of a
923   deep-sea hydrothermal mussel assemblage monitored by the EMSO-Açores MoMAR
924   observatory. Deep-Sea Res Pt I 90:62–75. doi: 10.1016/j.dsr.2014.04.004
925   Sarrazin J, Legendre P, de Busserolles F, Fabri M-C, Guilini K, Ivanenko VN, Morineaux M,
926   Vanreusel A, Sarradin P-M (2015) Biodiversity patterns, environmental drivers and
927   indicator species on a high-temperature hydrothermal edifice, Mid-Atlantic Ridge. Deep-
928   Sea Res Pt II 121:177–192. doi: 10.1016/j.dsr2.2015.04.013
929   Sasaki T, Warén A, Kano Y, Okutani T, Fujikura K (2010) Gastropods from Recent Hot Vents
930   and Cold Seeps: Systematics, Diversity and Life Strategies. In: Kiel S (ed) The Vent and
931   Seep Biota: Aspects from Microbes to Ecosystems. Springer Netherlands, Dordrecht, pp
932   169–254
933   Schneider CA, Rasband WS, Eliceiri KW (2012) NIH Image to ImageJ: 25 years of image
934   analysis. Nat Methods 9:671–675. doi: 10.1038/nmeth.2089
935   Shank TM, Fornari DJ, Von Damm KL, Lilley MD, Haymon RM, Lutz RA (1998) Temporal and
936   spatial patterns of biological community development at nascent deep-sea
937   hydrothermal vents (9°50'N, East Pacific Rise). Deep-Sea Res Pt II 45:465–515. doi:
938   10.1016/S0967-0645(97)00089-1
939   Sheader M, Van Dover CL, Shank TM (2000) Structure and function of *Halice hesmonectes*
940   (Amphipoda: Pardaliscidae) swarms from hydrothermal vents in the eastern Pacific. Mar
941   Biol 136:901–911. doi: 10.1007/s002270000300
942   Sheader M, Van Dover CL, Thurston MH (2004) Reproductive ecology of *Bouvierella*
943   *curtirama* (Amphipoda: Eusiridae) from chemically distinct vents in the Lucky Strike vent
944   field, Mid-Atlantic Ridge. Mar Biol 144:503–514. doi: 10.1007/s00227-003-1211-8
945   Sievert SM, Ziebis W, Kuever J, Sahm K (2000) Relative abundance of Archaea and Bacteria
946   along a thermal gradient of a shallow-water hydrothermal vent quantified by rRNA slot-
947   blot hybridization. Microbiol 146 (Pt 6):1287–1293. doi: 10.1099/00221287-146-6-1287
948   Smith CR, Kukert H, Wheatcroft RA, Jumars PA, Deming JW (1989) Vent fauna on whale
949   remains. Nature 341:27–28. doi: 10.1038/341027a0
950   Suzuki K, Yoshida K, Watanabe H, Yamamoto H (2018) Mapping the resilience of
951   chemosynthetic communities in hydrothermal vent fields. Sci Rep 8:9364. doi:
952   10.1038/s41598-018-27596-7
953   Turnipseed M, Jenkins CD, Van Dover CL (2004) Community structure in Florida Escarpment
954   seep and Snake Pit (Mid-Atlantic Ridge) vent mussel beds. Mar Biol 145:121–132. doi:
955   10.1007/s00227-004-1304-z
956   Tyler PA, Billett DSM (1988) The Reproductive Ecology of Elasipodid Holothurians from the N.
957   E. Atlantic. Biological Oceanography 5:273–296. doi: 10.1080/01965581.1987.10749518
958   Tyler PA, 1988. Seasonality in the deep-sea. Oceanogr Mar Biol. Annual Review 26: 227-258.
959   Tyler PA, Campos-Creasey, L.S. and Giles, L.A., 1994. Environmental control of quasi-
960   continuous and seasonal reproduction in deep-sea benthic invertebrates. In
961   Reproduction, Larval Biology and Recruitment of the Deep-Sea Benthos, edited by C. M.
962   Young and K. J. Eckelbarger. New York: Columb U Pr, pp. 158-178.
963   Tyler PA, Young CM (1999) Reproduction and dispersal at vents and cold seeps. J Mar Biol
964   Assoc UK 79:193–208. doi: 10.1017/S0025315499000235
965   Tyler PA, Pendlebury S, Mills SW, Mullineaux L, Eckelbarger KJ, Baker M, Young CM (2008)
966   Reproduction of Gastropods from Vents on the East Pacific Rise and the Mid-Atlantic

967 Ridge. J Shellfish Res. 27:107–118. doi: [10.2983/0730-](https://doi.org/10.2983/0730-8000(2008)27[107:ROGFVO]2.0.CO;2)
968 [8000(2008)27[107:ROGFVO]2.0.CO;2](https://doi.org/10.2983/0730-8000(2008)27[107:ROGFVO]2.0.CO;2)

969 Van Dover CL (2014) Impacts of anthropogenic disturbances at deep-sea hydrothermal vent
970 ecosystems: A review. Mar Environ Res 102:59–72. doi:
971 [10.1016/j.marenvres.2014.03.008](https://doi.org/10.1016/j.marenvres.2014.03.008)

972 Van Dover CL, Trask J, Gross J, Knowlton A (1999) Reproductive biology of free-living and
973 commensal polynoid polychaetes at the Lucky Strike hydrothermal vent field (Mid-
974 Atlantic Ridge). Mar Ecol Progr Ser 181:201–214. doi: [10.3354/meps181201](https://doi.org/10.3354/meps181201)

975 Vic C, Gula J, Roullet G, Pradillon F (2018) Dispersion of deep-sea hydrothermal vent effluents
976 and larvae by submesoscale and tidal currents. Deep-Sea Res Pt I 133:1–18. doi:
977 [10.1016/j.dsr.2018.01.001](https://doi.org/10.1016/j.dsr.2018.01.001)

978 Vrijenhoek RC (2010) Genetic diversity and connectivity of deep-sea hydrothermal vent
979 metapopulations. Mol Ecol 19:4391–4411. doi: [10.1111/j.1365-294X.2010.04789.x](https://doi.org/10.1111/j.1365-294X.2010.04789.x)

980 Warén A, Bouchet P (2001) Gastropoda and Monoplacophora from hydrothermal vents and
981 seeps ; new taxa and records. The Veliger 44:116–231.

982 Warèn A, Bouchet P (1993) New records, species, genera, and a new family of gastropods
983 from hydrothermal vents and hydrocarbon seeps. Zool Scr 22:1–90. doi: [10.1111/j.1463-](https://doi.org/10.1111/j.1463-6409.1993.tb00342.x)
984 [6409.1993.tb00342.x](https://doi.org/10.1111/j.1463-6409.1993.tb00342.x)

985 Warén A (1996) New and little known mollusca from Iceland and Scandinavia. Part 3. Sarsia
986 81:197–245. doi: [10.1080/00364827.1996.10413622](https://doi.org/10.1080/00364827.1996.10413622)

987 Watanabe H, Kado R, Kaida M, Tsuchida S, Kojima S (2006) Dispersal of vent-barnacle (genus
988 Neoverruca) in the Western Pacific. Cah Biol Mar 47: 353–357

989 Watanabe H, Fujikura K, Kinoshita G et al (2009) Egg capsule of *Phymorhynchus buccinoides*
990 (Gastropoda: Turridae) in a deep-sea methane seep site in Sagami Bay, Japan. Venus
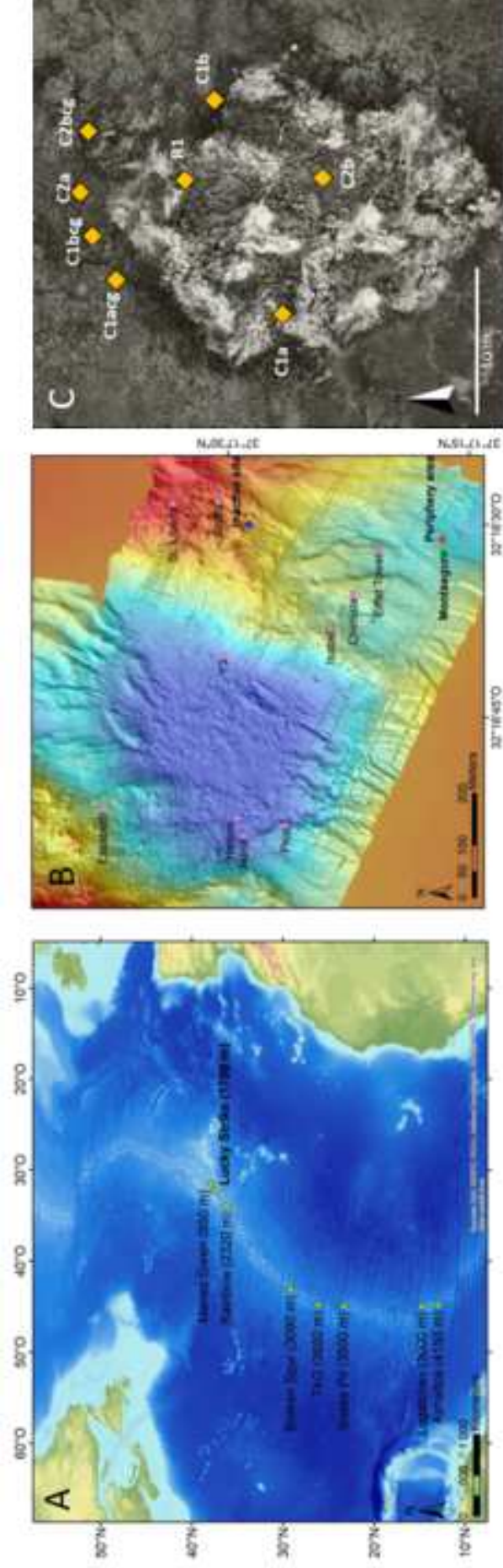991 67:181–188

992 Yahagi T, Watanabe HK, Kojima S, Kano Y (2017) Do larvae from deep-sea hydrothermal vents
993 disperse in surface waters? Ecology 98:1524–1534. doi: [10.1002/ecy.1800](https://doi.org/10.1002/ecy.1800)
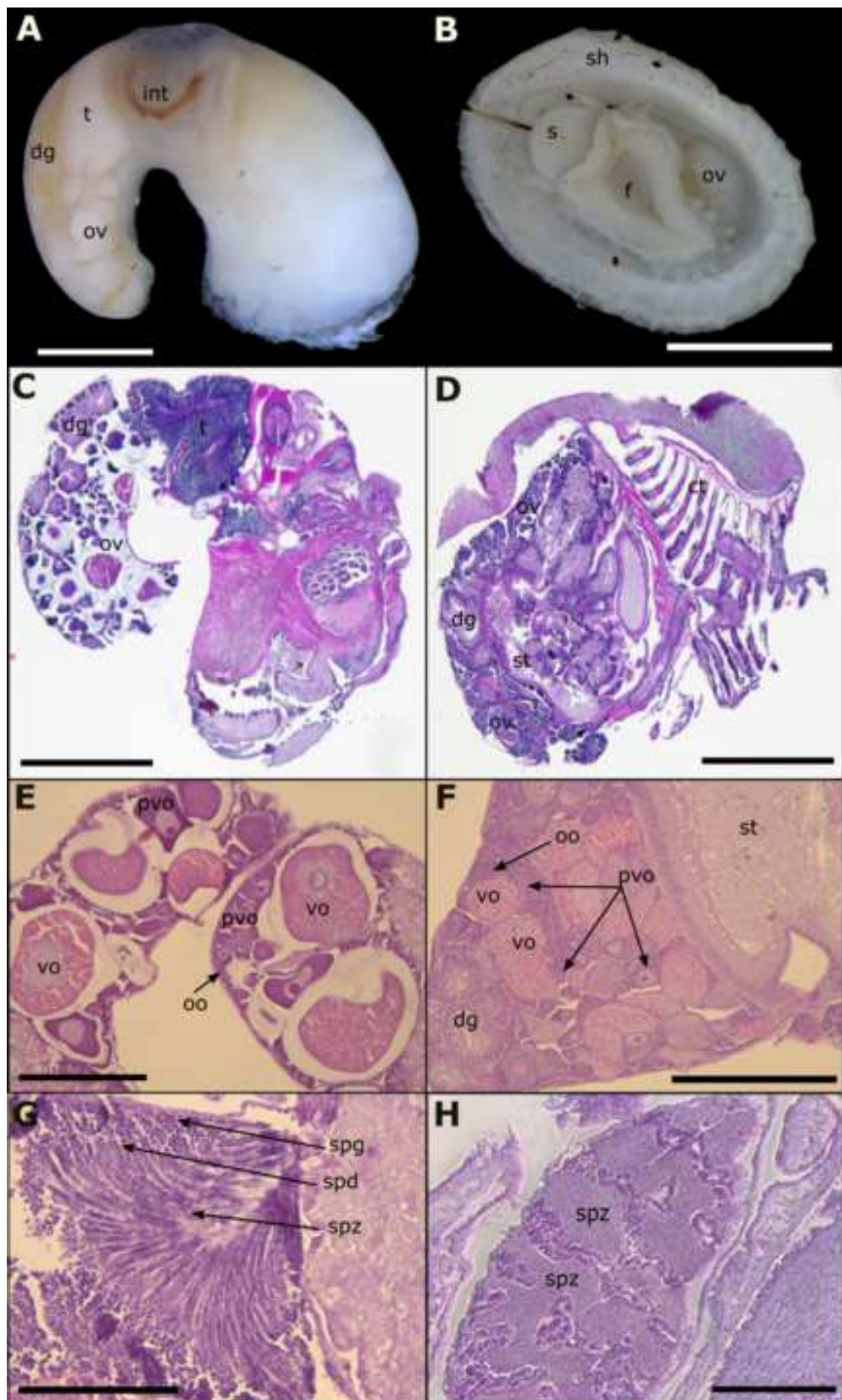
994 Young CM, Eckelbarger KJ, Eckelbarger K (1994) Reproduction, Larval Biology, and
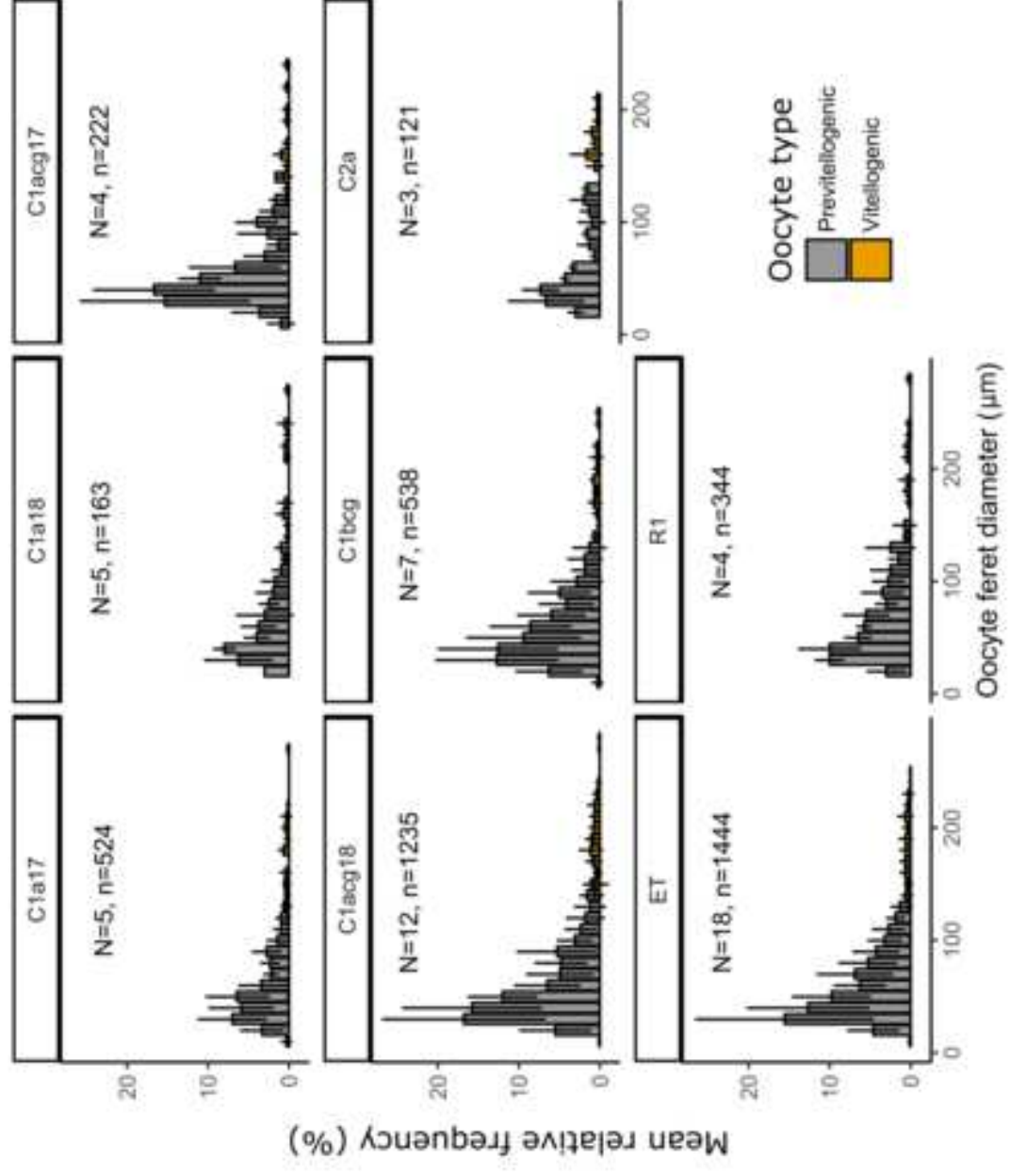995 Recruitment of the Deep-sea Benthos. Columb U Pr

996 Young CM. (2003) Reproduction, Development and Life History Traits, in: Ecosystems of the
997 World, Vol. 28, Ecosystems of the Deep Oceans, edited by: Tyler, P. A., Elsevier, London,
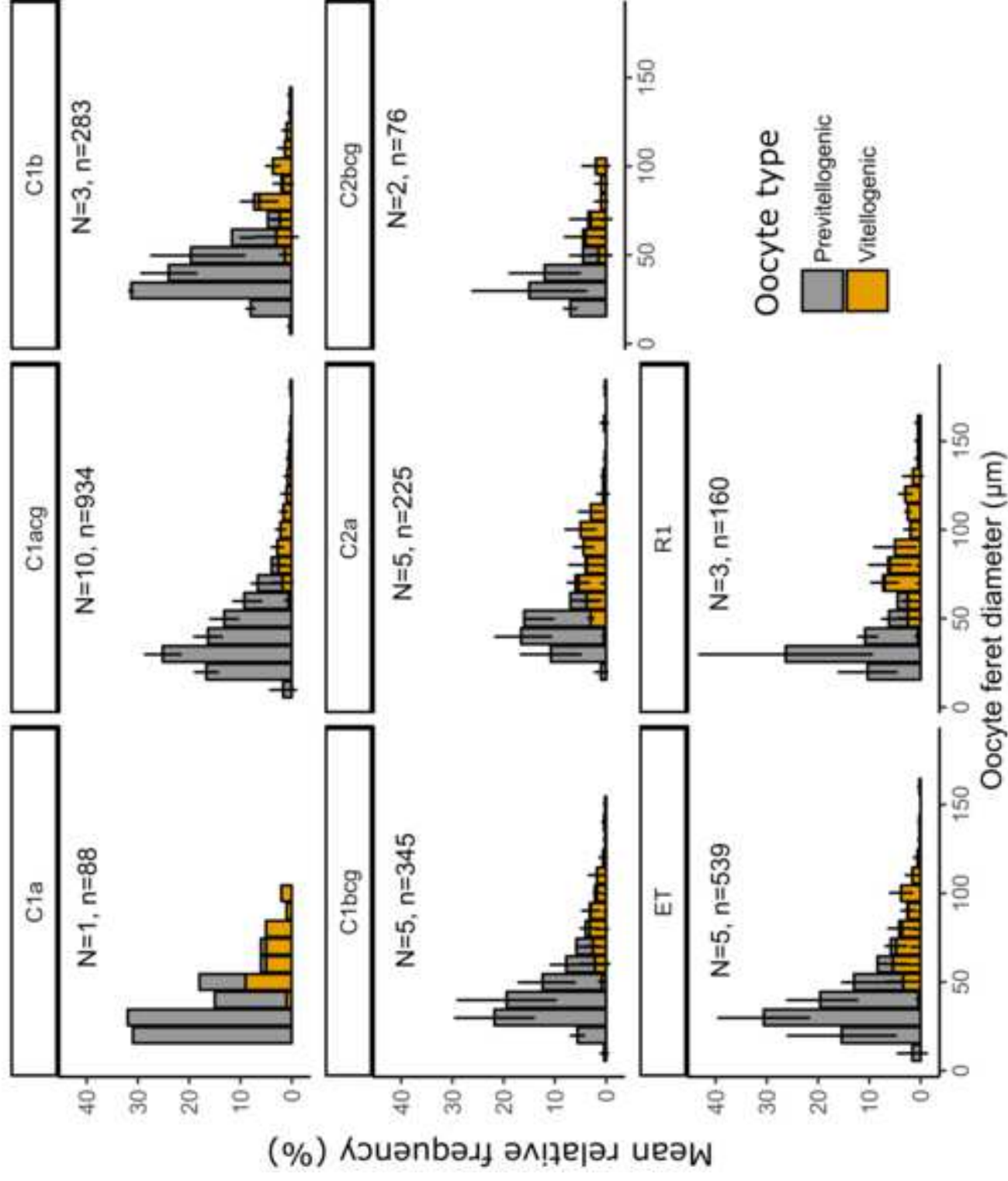998 381–426

999 Zal F, Jollivet D, Chevaldonné P, Desbruyères D (1995) Reproductive biology and population
1000 structure of the deep-sea hydrothermal vent worm *Paralvinella grasslei* (Polychaeta:
1001 Alvinellidae) at 13°N on the East Pacific Rise. Mar Biol122:637–648. doi:
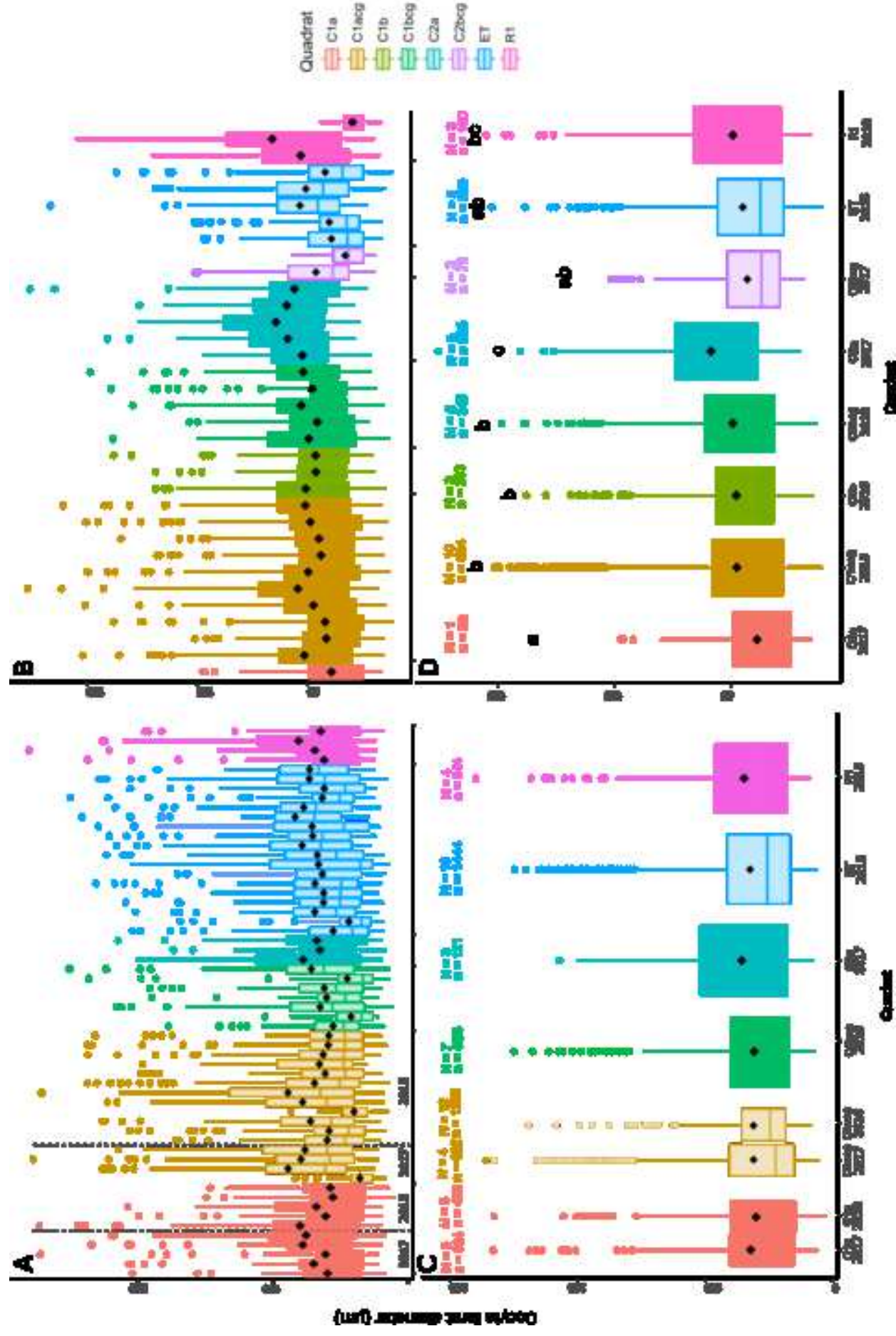1002 [10.1007/BF00350685](https://doi.org/10.1007/BF00350685)

1003 Zar JH (2007) Biostatistical Analysis (5th Edition). Prentice-Hall, Inc., Upper Saddle River, NJ,
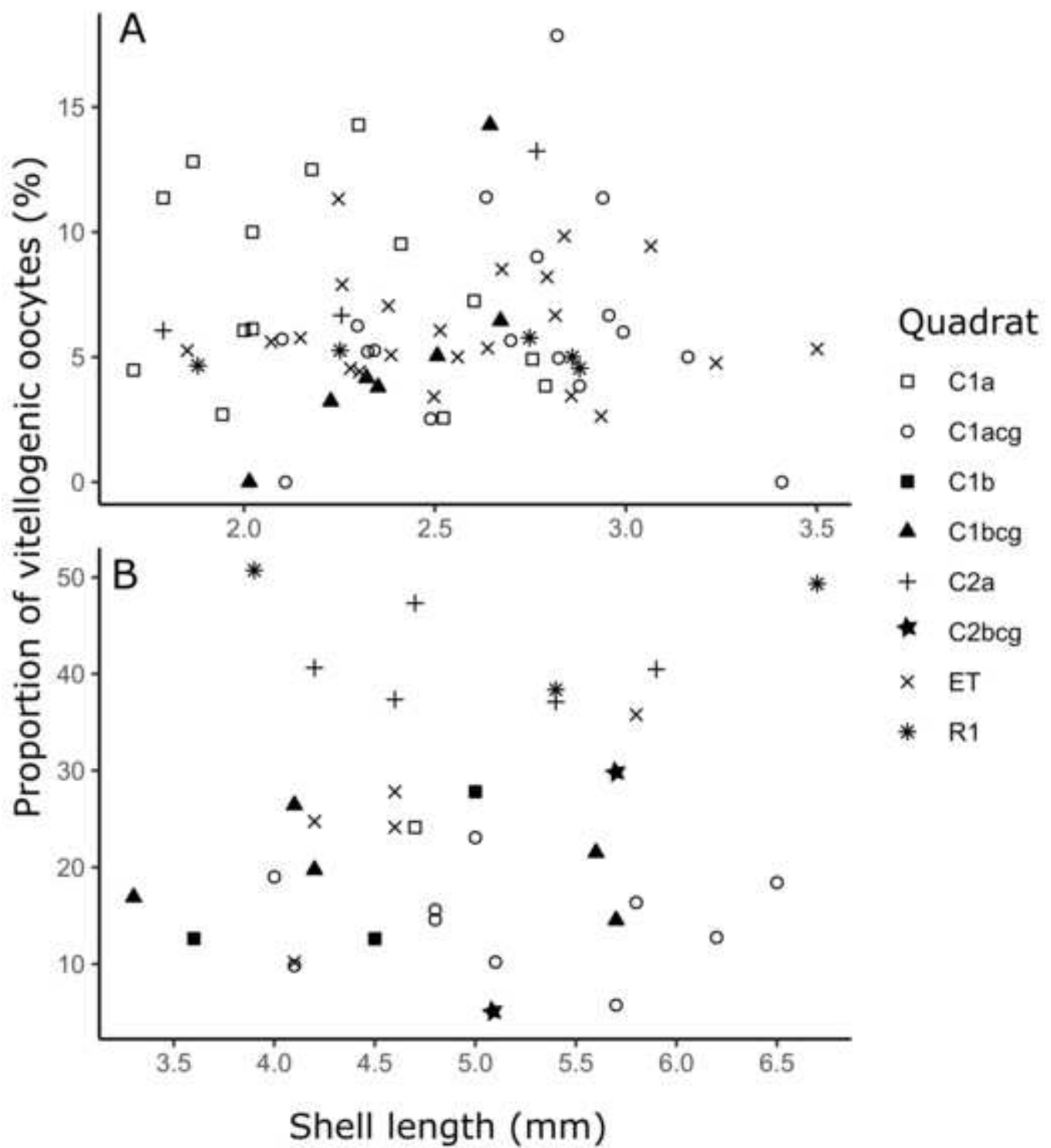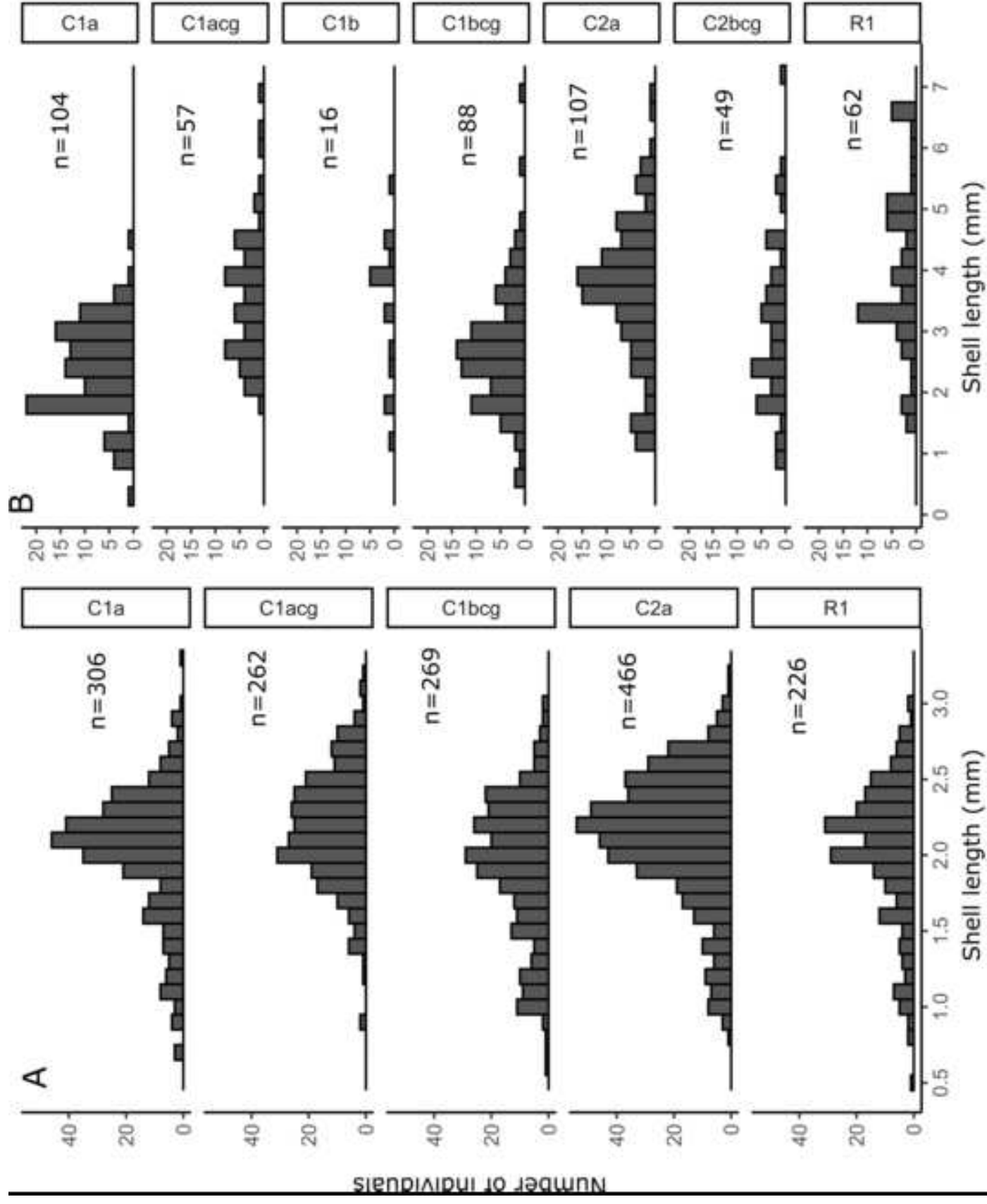1004 USA

Figure1

Figure2

Click here to access/download;Figure;Fig2.png ⬇

Figure3

Figure4

Figure5
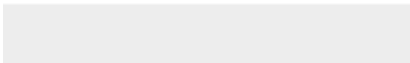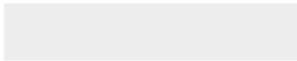
Figure6

Figure7

Figure S1

Click here to access/download
Supplementary Material
FigS1.png

Figure S2

Click here to access/download
Supplementary Material
FigS2.png